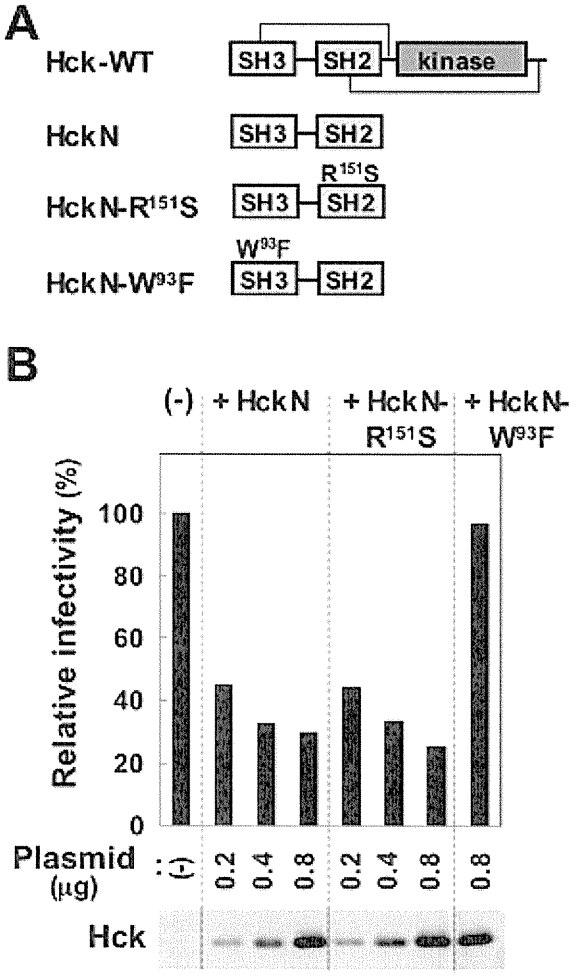

Figure 6. The effects of the overexpression of mutant forms of Hck on viral infectivity. (A) The mutant forms of Hck used are shown schematically. HckN lacks the kinase domain and the two intramolecular interactions present in the wild-type (WT) Hck. HckN-based HckN-R151S and HckN-W93F have amino acid substitutions in their SH2 and SH3 domain, respectively. (B) The 293 cells were transfected with the NL43 wild-type proviral plasmid or co-transected with the indicated amount of plasmid (HckN, HckN-R151S, or HckN-W93F). The infectivity of the viruses produced in the supernatants was determined using TZM-bl cells as the target cells and is expressed as a percentage of the value for the sample on the far left (bar graph). The amount of p24 inoculated was 8 ng/ml. Alternatively, the producer 293 cells were lysed and analyzed for the expression of the mutant Hck proteins by Western blotting (blot).
doi:10.1371/journal.pone.0027696.g006

underlined). On the other hand, molecular modeling also identified several residues in Nef that are responsible for its binding to Hck, such as P72, P75, R77, A83, F90, W113, His116, and Y120 [38]. Among them, R77, A83, F90, and Y120 were also found in the 2c-Nef docking model (Fig. 9, underlined), supporting the finding that 2c inhibits the binding of Hck to Nef or Nef PxxP motif-derived peptides (Figs. 7C and 8B). In summary, the present study revealed that the compound 2c reduced the infectivity of HIV-1 viruses and suggested that its inhibitory activity is mediated by its direct binding to Nef.

It remains to be determined exactly how 2c reduces Nef-mediated infectivity enhancement. Given that both 2c and the Hck SH3 domain bind directly to overlapping domains of Nef and reduce viral infectivity, we speculate that their inhibitory effects are due to the inhibition of the interaction of Nef with host proteins (Fig. 10). One of the candidates for such a host protein is p21-activated kinase 2, PAK2, the association of which depends on the Nef PxxP motif [39]. However, we did not observe any inhibitory effect of 2c on the association of Nef with PAK2 activity or its downstream effector functions (data not shown), and the Nef-PAK2 association is dispensable for the enhancement of infectivity by the viral protein [40]. Another candidate is the GTPase dynamin 2 whose interaction with Nef was implicated in enhancing viral infectivity [41]. However, again, we did not observe any significant inhibitory effect of 2c on the binding of Nef to dynamin 2, which was assessed using a co-immunoprecipitation assay (data not shown). Thus, the inhibitory activity of 2c observed in this study appears to be independent of these host proteins. The inhibitory compound 2c is a useful chemical probe for investigating the underlying molecular mechanism by which Nef enhances the infectivity of HIV-1, and in particular, for identifying the host proteins involved in the process.

Recently, a single-domain antibody (sdAb) that binds to Nef was reported [42]. Although the binding domains in Nef remained unclear, anti-Nef sdAb was also shown to reduce *in vitro* viral infectivity [42]. Therefore, to clarify whether viral infectivity enhancement by Nef accounts for the high *in vivo* viral load observed in the presence of Nef, it is necessary to test the effects of 2c, a more potent analog, and/or the anti-Nef sdAb in animal models such as HIV-1-infected humanized mice.

Materials and Methods

The compound 2c preparation

Some of the 2c was prepared by Kyowa Hakko Kogyo (Tokyo, Japan), as described previously [43], whilst the rest (a large quantity) was prepared by Sai Advantium Pharma (Hyderabad, India). Both preparations were dissolved in DMSO and had an equivalent inhibitory effect on HIV-1 infectivity (data not shown).

Proviral plasmids

The provial NL43 plasmid and its derivatives, which had mutations in the Nef gene (ΔNef, R77A, K82A, D86A, F90A, and G119L), were prepared as described previously [35]. The Env-defective mutant (pNL-Kp) and VSV-G expression plasmid were prepared as described previously [44]. The proviral JRFL plasmid was provided by Y. Koyanagi (Kyoto University, Kyoto, Japan) [45]. We also prepared the proviral JRFL plasmid, in which the Nef gene was disrupted (ΔNef) or replaced with the PxxP motif-disrupted AxxA mutant [30].

Hck plasmids

The p56Hck cloned into the pcDNA3.1 vector (Invitrogen) was prepared as described previously [18]. The mutant forms of Hck cloned into the pCAGGS vector (HckN, Hck-R151S, and Hck-W93F; see Fig. 6A) were provided by M. Matsuda (Kyoto University, Kyoto, Japan) [37].

GST fusion plasmids

The control GST and GST-Nef fusion plasmids (the wild-type NL43, NL43 Nef-TR mutant, NL43 Nef-AxxA, and the wild-type SF2; see Fig. 7) were prepared as described previously [30]. We also prepared a GST-SF2 Nef-PxxP plasmid, which expressed a 20-mer peptide derived from the PxxP motif of SF2 Nef (see Fig. 8). The cDNA containing the motif was amplified by PCR using the following primers (5′-GGATCCGTGGGTTTTCCAGT-3′ and 5′-GTCGACCTATAAAGCTGCCT-3′), cloned into the pCR2.1 vector (Invitrogen), sequenced using the BigDye Terminator v3.1

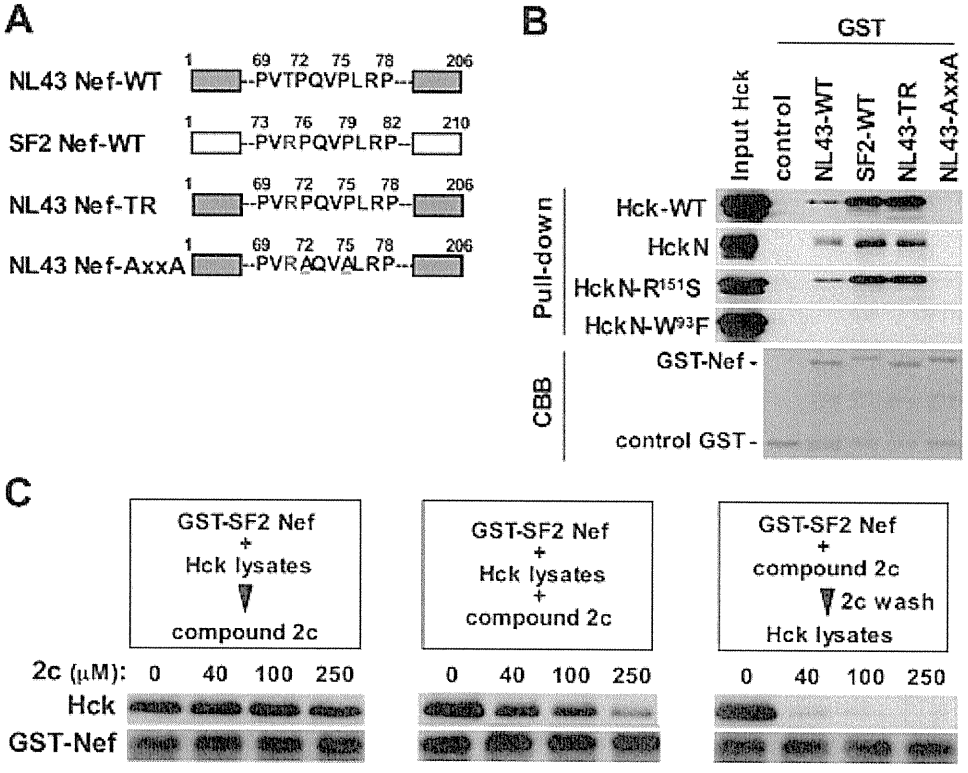

Figure 7. The effect of 2c on binding between Nef and Hck. (A) The Nef proteins fused to GST are shown schematically. In addition to the wild-type (WT) SF2 and NL43 strain Nef, the NL43-TR mutant, which contained a T71R amino acid substitution, and another NL43 AxxA mutant, in which the PxxP motif was disrupted (P72A and P75A substitutions), were used. (B) The resins to which the control GST or indicated GST-Nef fusion proteins were bound were incubated with the lysates of 293 cells expressing the indicated Hck protein. The amount of Hck bound to the resins was determined by Western blotting (pull-down assay). To confirm the equal expression of these Hck proteins in the 293 cells, equal amounts of each cell lysate were analyzed (Input Hck). Moreover, the amounts of the GST and GST-Nef fusion proteins bound to the resins were verified by the elution from the resins followed by SDS-PAGE/Coomassie brilliant blue (CBB) staining. (C) Three different competitive pull-down assays were performed. In the experiment shown in the left panel, the resins to which the GST-SF2 Nef fusion proteins were bound were incubated with the lysates obtained from the 293 cells expressing the wild-type Hck for 3 h, and then 2c was added to the mixture at the indicated concentration. In the experiment shown in the middle panel, the resins to which the GST-SF2 Nef fusion proteins were bound were incubated with the lysates of 293 cells expressing the wild-type Hck and the indicated concentration of 2c. In the experiment shown in the right panel, the resins to which the GST-SF2 Nef fusion proteins were bound were first incubated with the indicated concentration of 2c for 4 h and then washed to remove unbound 2c. Then, the resins were incubated with the lysates of 293 cells expressing the wild-type Hck. The amount of Hck bound to the resins was determined by Western blotting (upper blots). The GST-Nef blot was used as a loading control (lower blots). Data shown are representative of two independent experiments with similar results.
doi:10.1371/journal.pone.0027696.g007

Cycle Sequencing kit (Applied Biosystems) and the ABI PRISM 3100 Genetic Analyzer (Applied Biosystems), and cloned into the pGEX-6P-1 bacterial expression vector (GE Healthcare).

Virus preparation

HEK293 cells (Invitrogen) were maintained in DME medium supplemented with 10% FCS and used as viral producer cells. The 293 cells were seeded onto 12-well tissue culture plates at a density of 1.8×10^5 cells/well and transfected with 1.6 μg/well of various proviral HIV-1 plasmids using 4 μl/well Lipofectamine 2000 reagent (Invitrogen). To prepare VSV-G-pseudotyped viruses (see Fig. 2C), cells were transfected with 0.5 μg/well Env-defective mutant plasmid (pNL-Kp) and 1.0 μg/well VSV-G expression plasmid. In a selected experiment (see Fig. 6B), the cells were co-transfected with 0.8 μg/well pNL43 plasmid and 0.2, 0.4, or 0.8 μg/well of one of the mutant forms of Hck (HckN, HckN-R151S, or HckN-W93F). The total amount (1.6 μg/well) of the plasmid was normalized using the pCAGGS empty vector. After 6 h of transfection, the culture medium was replaced with fresh medium, and the cells were cultured for an additional 48 h in the presence or absence of 2c at the indicated concentrations. In a selected experiment (see Fig. 2B), 2c was added to the culture 24 h after transfection. Then, the supernatants containing the viruses were clarified by brief centrifugation, and viral production was assessed by measuring the concentration of p24 Gag protein in the supernatants using the RETROtek p24 Antigen ELISA kit (ZeptoMetrix). Viral production was also assessed by analyzing the expression of viral proteins in the cells by Western blotting. The preparation of the total cell lysates and Western blotting were performed essentially as described previously [17,18,30]. Briefly, the cells were lysed on ice with Nonidet P-40 lysis buffer (1% Nonidet P-40, 50 mM Tris, and 150 mM NaCl) containing protease inhibitors (1 mM EDTA, 1 μM PMSF, 1 μg/ml aprotinin, 1 μg/ml leupeptin, and 1 μg/ml pepstatin). Total cell lysates were then subjected to Western blotting. The antibodies used were as follows: anti-Gag (#65-004; BioAcademia, Osaka, Japan), anti-Nef (#2949; NIH AIDS Research & Reference Program), anti-Vif (#319; NIH AIDS Research & Reference Program), and anti-actin (#C-2; Santa Cruz). The detection was performed with HRP-labeled secondary antibodies (GE Health-

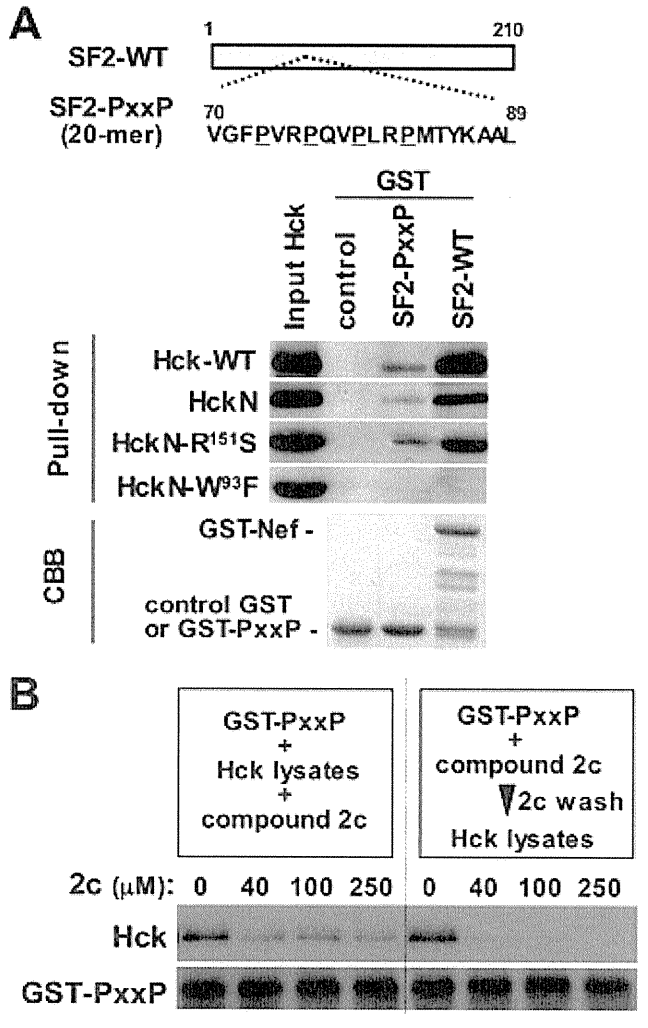

Figure 8. The effect of 2c on the binding between Nef PxxP motif-containing peptides and Hck. (A) The Nef peptide fused to GST is shown schematically. The 20 amino acid peptide derived from the PxxP motif of SF2 Nef was used (the proline residues are underlined). The resins to which the control GST, GST-SF2 Nef-PxxP peptides (SF2-PxxP), or GST-intact SF2 Nef (SF2-WT) fusion proteins were bound were incubated with the lysates of 293 cells expressing the indicated Hck protein. The amount of Hck bound to each resin was determined by Western blotting (Pull-down). To verify the equal expression of these Hck proteins in the 293 cells, equal amounts of each cell lysate were analyzed (Input Hck). Moreover, the amounts of the GST and GST-Nef fusion proteins bound to the resins were verified by eluting from the resins followed by SDS-PAGE/Coomassie brilliant blue (CBB) staining. (B) Two different competitive pull-down assays were performed. In the experiment shown in the left panel, the resins to which the GST-SF2 Nef-PxxP peptides were bound were incubated with the lysates of 293 cells expressing the wild-type Hck and the indicated concentration of 2c. In the experiment shown in the right panel, the resins to which the GST-SF2 Nef-PxxP peptides were bound were incubated with the indicated concentrations of 2c for 4 h and then washed to remove unbound 2c. Then, the resins were incubated with the lysates of 293 cells expressing the wild-type Hck. The amount of Hck bound to the resins was determined by Western blotting (upper blots). The GST-Nef blot was used as a loading control (lower blots). Data shown are representative of two independent experiments with similar results.
doi:10.1371/journal.pone.0027696.g008

care), the Immunostar LD Western blotting detection reagent (Wako, Osaka, Japan), and an image analyzer (ImageQuant LAS 4000; GE Healthcare).

Infectivity assay

TZM-bl cells (NIH AIDS Research & Reference Program) were maintained in DME medium supplemented with 10% FCS and used as viral target cells. TZM-bl cells were seeded onto 96-well tissue culture plates at a density of 6×10^3 cells/well and challenged with serially diluted viruses normalized for the concentration of p24 Gag protein. The supernatant of the proviral plasmid-transfected 293 cells was used as a viral stock and diluted with DME medium containing 10% FCS and 20 μg/ml DEAE-dextran (MP Biomedicals, Solon, OH). The diluted viruses were then added to the target cells (150 μl/well) overnight, and the culture medium was replaced with fresh DME medium containing 10% FCS and incubated for 48 h. In a selected experiment (see Fig. 2A), 2c was added to TZM-bl cells together with the diluted viruses. Viral infectivity was assessed by measuring the HIV-1 Tat-mediated induction of β-galactosidase activity in the target cells using a β-Galactosidase Enzyme Assay System (Promega). The absorbance of the wells was measured at 420 nm using a Multiskan microplate reader (Thermo Electron).

Replication assay

The replication assay with macrophages was performed essentially as described previously [46]. Heparinized venous blood was collected from healthy donors, after informed consent was obtained in accordance with the Declaration of Helsinki. The approval for this study was obtained from the Kumamoto University Medical Ethical Committee. Mononuclear cells obtained using LSM reagent (MP Biomedicals) were suspended into RPMI1640 medium-1% FCS at 1×10^6 cells/ml and seeded into 24-well plates. Monocytes were enriched by adherence to plates for 1 h at 37°C, and non-adherent cells were removed by extensive washing with PBS. Then, the adherent monocytes were differentiated into macrophages by culturing with RPMI1640-10% FCS containing 100 ng/ml rhM-CSF (a gift from Morinaga Milk Industry, Kanagawa, Japan). After 3 days, the cultures were replaced with fresh complete media and incubated for another 3 days. The purity of the day 6-macrophages prepared by this method was routinely more than 95% when assessed by the expression of CD14 (data not shown). Then, macrophages were incubated with 250 μl of the 293 cell supernatants containing JRFL HIV-1 viruses for 2 h at 37°C. Either 2c or DMSO was added to the incubation together with the diluted viruses. AZT (NIH AIDS Research & Reference Program) was used as a positive control. The cells were washed twice with PBS to remove unbound viruses and cultured with RPMI1640-10% FCS containing rhM-CSF in the presence or absence of 2c or AZT. One-half of the culture media was replaced with the complete media every 3 days. The culture supernatants collected at day 6, 9 and 12 were analyzed for the concentration of p24 Gag proteins by ELISA to monitor viral replication.

Jurkat cells were also used in this study. The cell pellet (1×10^6 cells) were incubated with 500 μl of the 293 cell supernatants containing NL43 viruses for 2 h at 37°C. Either 2c or DMSO was added to the incubation together with the diluted viruses. AZT was used as a positive control. The cells were washed twice with PBS, resuspended into 1 ml of RPMI1640-10% FCS, and cultured for 3 days in the presence or absence of 2c or AZT. Then, the culture were diluted (1/5) with RPMI1640-10% FCS, and cultured for another 2 days in the presence or absence of 2c or AZT. The concentration of p24 in the culture supernatants of day 5, 7 and 9 was analyzed as above.

GST pull-down assay

The control GST and GST-Nef fusion proteins cloned in the pGEX-6P-1 vector were expressed in *E. coli* BL21 cells

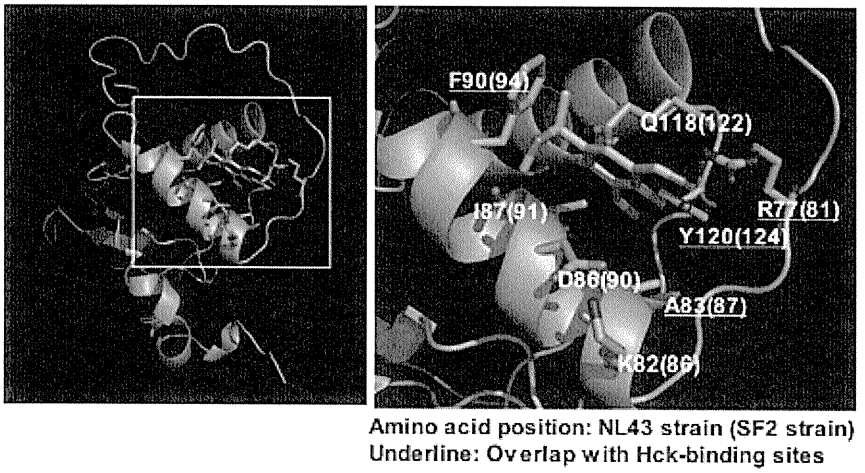

Figure 9. The 2c-Nef docking model. The amino acids that are predicted to be involved in the interaction between Nef and 2c are indicated. The positions of these amino acids in the NL43 strain and SF2 strain are shown. The amino acids predicted to interact with the Hck SH3 domain are underlined [38].
doi:10.1371/journal.pone.0027696.g009

(GE Healthcare). The cells were grown in LB medium containing 50 μg/ml ampicillin, before being induced with 1 μM IPTG (Sigma). The expression-induced cells were harvested and lysed with BugBuster Protein Extraction Reagent containing 1 U/ml rLysozyme and 25 U/ml Benzonase Nuclease (all from Novagen). The cleared lysates were then incubated with GST-Bind Resin (Novagen). After extensive washing with GST Bind/Wash Buffer (Novagen), the resin was incubated with the total cell lysate of the 293 cells transfected with the expression plasmid for Hck for 12 h. In the competitive pull-down assay, we employed the following 3 protocols: (1) the concurrent addition of 2c and Hck-containing lysates to the GST-Nef-bound resin, (2) the addition of Hck-containing lysates for 3 h followed by the addition of 2c, (3) the addition of 2c at the indicated concentrations for 4 h followed by the addition of the Hck-containing lysates. The incubation of the above mixtures was carried out at 4°C in Nonidet P-40 lysis buffer (1% Nonidet P-40, 50 mM Tris, and 150 mM NaCl) containing protease inhibitors (1 mM EDTA, 1 μM PMSF, 1 μg/ml aprotinin, 1 μg/ml leupeptin, and 1 μg/ml pepstatin). After extensive re-washing with complete Nonidet P-40 lysis buffer, the resin was boiled with SDS-PAGE sample buffer, and the eluates were analyzed for the presence of Hck by Western blotting with anti-Hck antibodies (clone 18; Transduction Laboratories).

The 2c-Nef docking model

We predicted the complex structures of Nef and 2c by homology modeling and docking simulation using the Molecular Operating Environment (MOE) ver. 2007.09. (Chemical Computing Group, Canada). First, homology modeling [47–49] was used to construct the model structure of HIV-1 Nef SF2 strain using its NMR structure (PDB code: 2NEF) [50] as a template. During the modeling, energy calculations were performed with the AMBER ff99 force field [51] and the GB/VI implicit solvent energy function [52]. Next, docking simulation of 2c with the homology model of Nef was achieved with the ASEDock module [53]. The initial structure of 2c was generated with the Molecular Builder module. Then, we searched for the binding site of 2c with the Site-Finder module. During the simulation, the energy calculations were performed with the MMFF94x force field [54,55] and the GB/VI implicit solvent energy function [52].

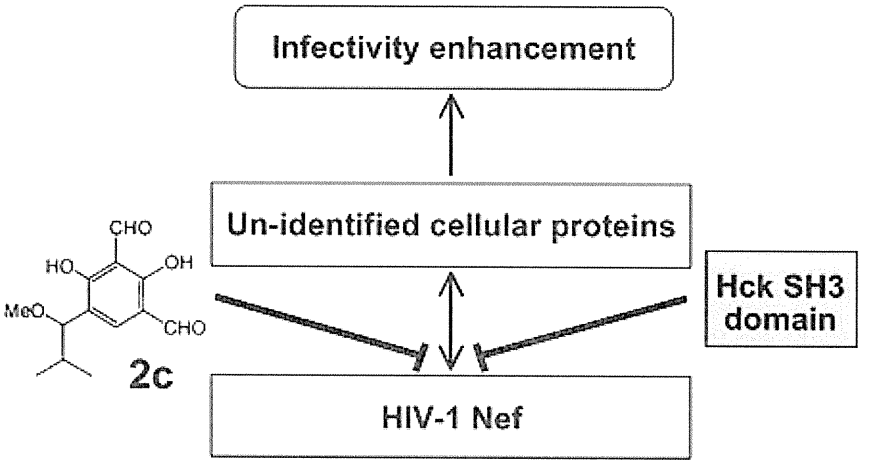

Figure 10. A model of the inhibitory effect of 2c. Both 2c and the Hck SH3 domain bind directly to Nef and reduce viral infectivity, probably by inhibiting the interaction of Nef with an unidentified cellular protein(s).
doi:10.1371/journal.pone.0027696.g010

During the docking simulation, movement of the main chain atoms around 4.5 Å of the ligand binding site in Nef was restrained with a harmonic potential of 100 kcal/mol/Å^2, while the atoms in compound 2c were not constrained. In this study, the structure with the lowest score was selected for the model.

Statistical analysis

The statistical significance of differences between assay groups was determined using Mann-Whitney U test. p values less than 0.05 were considered significant.

Acknowledgments

We thank F. Koutaki for her secretarial assistance.

Author Contributions

Conceived and designed the experiments: NC SS. Performed the experiments: NC MH HO HS OF PM. Analyzed the data: NC SO SS. Contributed reagents/materials/analysis tools: TU AA. Wrote the paper: NC SS.

References

1. Fackler OT, Baur AS (2002) Live and let die: Nef functions beyond HIV replication. Immunity 16: 493–497.
2. Peterlin BM, Trono D (2003) Hide, shield and strike back: how HIV-infected cells avoid immune eradication. Nat Rev Immunol 3: 97–107.
3. Foster JL, Garcia JV (2008) HIV-1 Nef: at the crossroads. Retrovirology 5: 84.
4. Malim MH, Emerman M (2008) HIV-1 accessory proteins–ensuring viral survival in a hostile environment. Cell Host Microbe 3: 388–398.
5. Deacon NJ, Tsykin A, Solomon A, Smith K, Ludford-Menting M, et al. (1995) Genomic structure of an attenuated quasi species of HIV-1 from a blood transfusion donor and recipients. Science 270: 988–991.
6. Kirchhoff F, Greenough TC, Brettler DB, Sullivan JL, Desrosiers RC (1995) Brief report: absence of intact nef sequences in a long-term survivor with nonprogressive HIV-1 infection. N Engl J Med 332: 228–232.
7. Hanna Z, Kay DG, Rebai N, Guimond A, Jothy S, et al. (1998) Nef harbors a major determinant of pathogenicity for an AIDS-like disease induced by HIV-1 in transgenic mice. Cell 95: 163–175.
8. Garcia JV, Miller AD (1991) Serine phosphorylation-independent downregulation of cell-surface CD4 by nef. Nature 350: 508–511.
9. Schaefer MR, Wonderlich ER, Roeth JF, Leonard JA, Collins KL (2008) HIV-1 Nef targets MHC-I and CD4 for degradation via a final common β-COP-dependent pathway in T cells. PLoS Pathog 4: e1000131.
10. Schwartz O, Maréchal V, Le Gall S, Lemonnier F, Heard JM (1996) Endocytosis of major histocompatibility complex class I molecules is induced by the HIV-1 Nef protein. Nat Med 2: 338–342.
11. Greenberg ME, Iafrate AJ, Skowronski J (1998) The SH3 domain-binding surface and an acidic motif in HIV-1 Nef regulate trafficking of class I MHC complexes. EMBO J 17: 2777–2789.
12. Williams M, Roeth JF, Kasper MR, Filzen TM, Collins KL (2005) Human immunodeficiency virus type 1 Nef domains required for disruption of major histocompatibility complex class I trafficking are also necessary for coprecipitation of Nef with HLA-A2. J Virol 79: 632–637.
13. Singh RK, Lau D, Noviello CM, Ghosh P, Guatelli JC (2009) An MHC-I cytoplasmic domain/HIV-1 Nef fusion protein binds directly to the μ subunit of the AP-1 endosomal coat complex. PLoS One 4: e8364.
14. Saksela K, Cheng G, Baltimore D (1995) Proline-rich (PxxP) motifs in HIV-1 Nef bind to SH3 domains of a subset of Src kinases and are required for the enhanced growth of Nef$^+$ viruses but not for downregulation of CD4. EMBO J 14: 484–491.
15. Moarefi I, LaFevre-Bernt M, Sicheri F, Huse M, Lee CH, et al. (1997) Activation of the Src-family tyrosine kinase Hck by SH3 domain displacement. Nature 385: 650–653.
16. Lerner EC, Smithgall TE (2002) SH3-dependent stimulation of Src-family kinase autophosphorylation without tail release from the SH2 domain in vivo. Nat Struct Biol 9: 365–369.
17. Suzu S, Harada H, Matsumoto T, Okada S (2005) HIV-1 Nef interferes with M-CSF receptor signaling through Hck activation and inhibits M-CSF bioactivities. Blood 105: 3230–3237.
18. Hiyoshi M, Suzu S, Yoshidomi Y, Hassan R, Harada H, et al. (2008) Interaction between Hck and HIV-1 Nef negatively regulates cell surface expression of M-CSF receptor. Blood 111: 243–250.
19. Vérollet C, Zhang YM, Le Cabec V, Mazzolini J, Charrière G, et al. (2010) HIV-1 Nef triggers macrophage fusion in a p61Hck- and protease-dependent manner. J Immunol 184: 7030–7039.
20. Chowers MY, Spina CA, Kwoh TJ, Fitch NJ, Richman DD, et al. (1994) Optimal infectivity in vitro of human immunodeficiency virus type 1 requires an intact nef gene. J Virol 68: 2906–2914.
21. Chowers MY, Pandori MW, Spina CA, Richman DD, Guatelli JC (1995) The growth advantage conferred by HIV-1 nef is determined at the level of viral DNA formation and is independent of CD4 downregulation. Virology 212: 451–457.
22. Aiken C, Trono D (1995) Nef stimulates human immunodeficiency virus type 1 proviral DNA synthesis. J Virol 69: 5048–5056.
23. Goldsmith MA, Warmerdam MT, Atchison RE, Miller MD, Greene WC (1995) Dissociation of the CD4 downregulation and viral infectivity enhancement functions of human immunodeficiency virus type 1 Nef. J Virol 69: 4112–4121.
24. Aiken C (1997) Pseudotyping human immunodeficiency virus type 1 (HIV-1) by the glycoprotein of vesicular stomatitis virus targets HIV-1 entry to an endocytic pathway and suppresses both the requirement for Nef and the sensitivity to cyclosporin A. J Virol 71: 5871–5877.
25. Chazal N, Singer G, Aiken C, Hammarskjöld ML, Rekosh D (2001) Human immunodeficiency virus type 1 particles pseudotyped with envelope proteins that fuse at low pH no longer require Nef for optimal infectivity. J Virol 75: 4014–4018.
26. Laguette N, Benichou S, Basmaciogullari S (2009) Human immunodeficiency virus type 1 Nef incorporation into virions does not increase infectivity. J Virol 83: 1093–1104.
27. Olszewski A, Sato K, Aron ZD, Cohen F, Harris A, et al. (2004) Guanidine alkaloid analogs as inhibitors of HIV-1 Nef interactions with p53, actin, and p56lck. Proc Natl Acad Sci U S A 101: 14079–14084.
28. Emert-Sedlak L, Kodama T, Lerner EC, Dai W, Foster C, et al. (2009) Chemical library screens targeting an HIV-1 accessory factor/host cell kinase complex identify novel antiretroviral compounds. ACS Chem Biol 4: 939–947.
29. Betzi S, Restouin A, Opi S, Arold ST, Parrot I, et al. (2007) Protein protein interaction inhibition (2P2I) combining high throughput and virtual screening: Application to the HIV-1 Nef protein. Proc Natl Acad Sci U S A 104: 19256–19261.
30. Hassan R, Suzu S, Hiyoshi M, Takahashi-Makise N, Ueno T, et al. (2009) Dysregulated activation of a Src tyroine kinase Hck at the Golgi disturbs *N*-glycosylation of a cytokine receptor Fms. J Cell Physiol 221: 458–468.
31. Dikeakos JD, Atkins KM, Thomas L, Emert-Sedlak L, Byeon IJ, et al. (2010) Small molecule inhibition of HIV-1-induced MHC-I downregulation identifies a temporally regulated switch in Nef action. Mol Biol Cell 21: 3279–3292.
32. Miller MD, Warmerdam MT, Gaston I, Greene WC, Feinberg MB (1994) The human immunodeficiency virus-1 nef gene product: a positive factor for viral infection and replication in primary lymphocytes and macrophages. J Exp Med 179: 101–113.
33. Spina CA, Kwoh TJ, Chowers MY, Guatelli JC, Richman DD (1994) The importance of nef in the induction of human immunodeficiency virus type 1 replication from primary quiescent CD4 lymphocytes. J Exp Med 179: 115–123.
34. Haller C, Tibroni N, Rudolph JM, Grosse R, Fackler OT (2011) Nef does not inhibit F-actin remodelling and HIV-1 cell-cell transmission at the T lymphocyte virological synapse. Eur J Cell Biol;in press.
35. Jere A, Fujita M, Adachi A, Nomaguchi M (2010) Role of HIV-1 Nef protein for virus replication in vitro. Microbes Infect 12: 65–70.
36. Madrid R, Janvier K, Hitchin D, Day J, Coleman S, et al. (2005) Nef-induced alteration of the early/recycling endosomal compartment correlates with enhancement of HIV-1 infectivity. J Biol Chem 280: 5032–5044.
37. Tokunaga K, Kiyokawa E, Nakaya M, Otsuka N, Kojima A, et al. (1998) Inhibition of human immunodeficiency virus type 1 virion entry by dominant-negative Hck. J Virol 72: 6257–6259.
38. Choi HJ, Smithgall TE (2004) Conserved residues in the HIV-1 Nef hydrophobic pocket are essential for recruitment and activation of the Hck tyrosine kinase. J Mol Biol 343: 1255–68.
39. Rauch S, Pulkkinen K, Saksela K, Fackler OT (2008) Human immunodeficiency virus type 1 Nef recruits the guanine exchange factor Vav1 via an unexpected interface into plasma membrane microdomains for association with p21-activated kinase 2 activity. J Virol 82: 2918–2929.
40. Schindler M, Rajan D, Specht A, Ritter C, Pulkkinen K, Saksela K, et al. (2007) Association of Nef with p21-activated kinase 2 is dispensable for efficient human immunodeficiency virus type 1 replication and cytopathicity in ex vivo-infected human lymphoid tissue. J Virol 81: 13005–13014.
41. Pizzato M, Helander A, Popova E, Calistri A, Zamborlini A, et al. (2007) Dynamin 2 is required for the enhancement of HIV-1 infectivity by Nef. Proc Natl Acad Sci U S A 104: 6812–6817.
42. Bouchet J, Basmaciogullari SE, Chrobak P, Stolp B, Bouchard N, et al. (2011) Inhibition of the Nef regulatory protein of HIV-1 by a single-domain antibody. Blood 117: 3559–3568.
43. Oneyama C, Agatsuma T, Kanda Y, Nakano H, Sharma SV, et al. (2003) Synthetic inhibitors of proline-rich ligand-mediated protein-protein interaction: potent analogs of UCS15A. Chem Biol 10: 443–451.
44. Akari H, Uchiyama T, Fukumori T, Iida S, Koyama AH, et al. (1999) Pseudotyping human immunodeficiency virus type 1 by vesicular stomatitis virus G protein does not reduce the cell-dependent requirement of vif for optimal

infectivity: functional difference between Vif and Nef. J Gen Virol 80: 2945–2959.
45. Koyanagi Y, Miles S, Mitsuyasu RT, Merrill JE, Vinters HV, et al. (1987) Dual infection of the central nervous system by AIDS viruses with distinct cellular tropisms. Science 236: 819–822.
46. Chihara T, Suzu S, Hassan R, Chutiwitoonchai N, Hiyoshi M, et al. (2010) IL-34 and M-CSF share the receptor Fms but are not identical in biological activity and signal activation. Cell Death Differ 17: 1917–1927.
47. Marti-Renom MA, Stuart AC, Fiser A, Sánchez R, Melo F, et al. (2000) Comparative protein structure modeling of genes and genomes. Annu Rev Biophys Biomol Struct 29: 291–325.
48. Baker D, Sali A (2001) Protein structure prediction and structural genomics. Science 294: 93–96.
49. Shirakawa K, Takaori-Kondo A, Yokoyama M, Izumi T, Matsui M, et al. (2008) Phosphorylation of APOBEC3G by protein kinase A regulates its interaction with HIV-1 Vif. Nat Struct Mol Biol 15: 1184–1191.
50. Grzesiek S, Bax A, Hu JS, Kaufman J, Palmer I, et al. (1997) Refined solution structure and backbone dynamics of HIV-1 Nef. Protein Sci 6: 1248–63.
51. Wang J, Cieplak P, Kollman PA (2000) How well does a restrained electrostatic potential (RESP) model perform in calcluating conformational energies of organic and biological molecules? J Comput Chem 21: 1049–1074.
52. Labute P (2008) The generalized Born/volume integral implicit solvent model: estimation of the free energy of hydration using London dispersion instead of atomic surface area. J Comput Chem 29: 1693–1698.
53. Goto J, Kataoka R, Muta H, Hirayama N (2008) ASEDock-docking based on alpha spheres and excluded volumes. J Chem Inf Model 48: 583–90.
54. Halgren TA (1999) MMFF VII. Characterization of MMFF94, MMFF94s, and other widely available force fields for conformational energies and for intermolecular-interaction energies and geometries. J Comput Chem 20: 720–29.
55. Halgren TA (1999) MMFF VI. MMFF94s option for energy minimization studies. J Comput Chem 20: 730–48.

frontiers in
MICROBIOLOGY

REVIEW ARTICLE
published: 29 December 2011
doi: 10.3389/fmicb.2011.00264

Structural dynamics of retroviral genome and the packaging

Yasuyuki Miyazaki*, Ariko Miyake, Masako Nomaguchi and Akio Adachi

Department of Microbiology, Institute of Health Biosciences, The University of Tokushima Graduate School, Tokushima, Japan

Edited by:
Mikako Fujita, Kumamoto University, Japan

Reviewed by:
Mikako Fujita, Kumamoto University, Japan
Jun-ichi Sakuragi, Osaka University, Japan

****Correspondence:***
Yasuyuki Miyazaki, Department of Microbiology, Institute of Health Biosciences, The University of Tokushima Graduate School, 3-18-15 Kuramoto, Tokushima 770-8503, Japan.
e-mail: ymiyazaki@basic.med.tokushima-u.ac.jp

Retroviruses can cause diseases such as AIDS, leukemia, and tumors, but are also used as vectors for human gene therapy. All retroviruses, except foamy viruses, package two copies of unspliced genomic RNA into their progeny viruses. Understanding the molecular mechanisms of retroviral genome packaging will aid the design of new anti-retroviral drugs targeting the packaging process and improve the efficacy of retroviral vectors. Retroviral genomes have to be specifically recognized by the cognate nucleocapsid domain of the Gag polyprotein from among an excess of cellular and spliced viral mRNA. Extensive virological and structural studies have revealed how retroviral genomic RNA is selectively packaged into the viral particles. The genomic area responsible for the packaging is generally located in the 5′ untranslated region (5′ UTR), and contains dimerization site(s). Recent studies have shown that retroviral genome packaging is modulated by structural changes of RNA at the 5′ UTR accompanied by the dimerization. In this review, we focus on three representative retroviruses, Moloney murine leukemia virus, human immunodeficiency virus type 1 and 2, and describe the molecular mechanism of retroviral genome packaging.

Keywords: retrovirus, genome, RNA, NC, structure, dimerization, packaging

INTRODUCTION

Retroviruses belong to a diverse family of RNA viruses causing various diseases, such as leukemia, tumors, demyelinization disease, and AIDS. One unique feature of retroviruses is their integration of reverse transcribed genome into the host chromosome as a provirus. Some retroviruses have been engineered to function as vectors for the delivery of corrective human genes, and vectors derived from the Moloney murine leukemia virus (MoMLV) have been used for the treatment of severe combined immunodeficiency (Nelson et al., 2003). An understanding of the molecular mechanism of retroviral replication is needed for the development of anti-retroviral therapies as well as retroviral vectors.

All retroviruses, except foamy viruses, package two copies of full-length genomic RNA into progeny viruses, the genomic RNA having to be specifically selected from among a large amount of spliced viral and cellular RNA (**Figure 1**; Berkowitz et al., 1996). Virological and genetic studies have shown that the specific packaging of retroviral genomic RNA is mediated via interaction with the nucleocapsid (NC) domain of the Gag polyprotein (Rein, 1994; Berkowitz et al., 1996; Jewell and Mansky, 2000; Greatorex, 2004; Paillart et al., 2004b; Russell et al., 2004). Retroviral NC domains are generally highly basic and contain one or two zinc knuckle motifs composed of C–C–H–C arrays (Henderson et al., 1981; Summers et al., 1990; Kodera et al., 1998; D'Souza and Summers, 2004; Matsui et al., 2007). The zinc knuckles form a metal-coordinating "reverse turn" stabilized by NH–S hydrogen bonds. Most retroviral zinc knuckles contain a hydrophobic cleft on the surface of the mini globular domain, recognizing specific structures of RNA or DNA. The basic N- and C-terminal tails of NC domains are conformationally labile (Summers et al., 1992).

Retroviral genomes are known to be non-covalently dimerized in progeny virions (Rizvi and Panganiban, 1993). The region responsible for retroviral genome packaging is generally located between the splice donor (SD) site and the *gag* start codon in the 5′ leader region (Watanabe and Temin, 1982; Mann and Baltimore, 1985; Lever et al., 1989; Mansky et al., 1995; Kaye and Lever, 1999; Browning et al., 2003; Mustafa et al., 2004). Interestingly, the packaging signal generally overlaps with the site of dimerization (Paillart et al., 1996, 2004a; Greatorex, 2004; Hibbert et al., 2004), implying that the packaging event is coupled with genome dimerization (Russell et al., 2004). Inhibition of genome dimerization by deletion or insertion mutations at dimer initiation sites (DIS) causes a drastic reduction in genome packaging (Berkhout, 1996; Paillart et al., 1996; Laughrea et al., 1997; McBride and Panganiban, 1997). Moreover, studies with mutant viruses containing two 5′ untranslated region (UTR) packaged monomeric genome, indicate that genome packaging is achieved by the interaction of two 5′ UTRs (Sakuragi et al., 2001, 2002). Experiments with MoMLV have indicated that the conformational change induced by genome dimerization causes the exposure of NC-binding sites (D'Souza and Summers, 2004). A recent study also indicated that human immunodeficiency virus type 1 (HIV-1) employs a similar strategy for genome packaging (Lu et al., 2011a). In addition, several structures have been determined among complexes of NC and RNA fragments functioning in genome packaging, which provide the molecular mechanism for retroviral genome recognition of NC at the atomic level. In this review, we describe the molecular mechanisms of retroviral genome packaging.

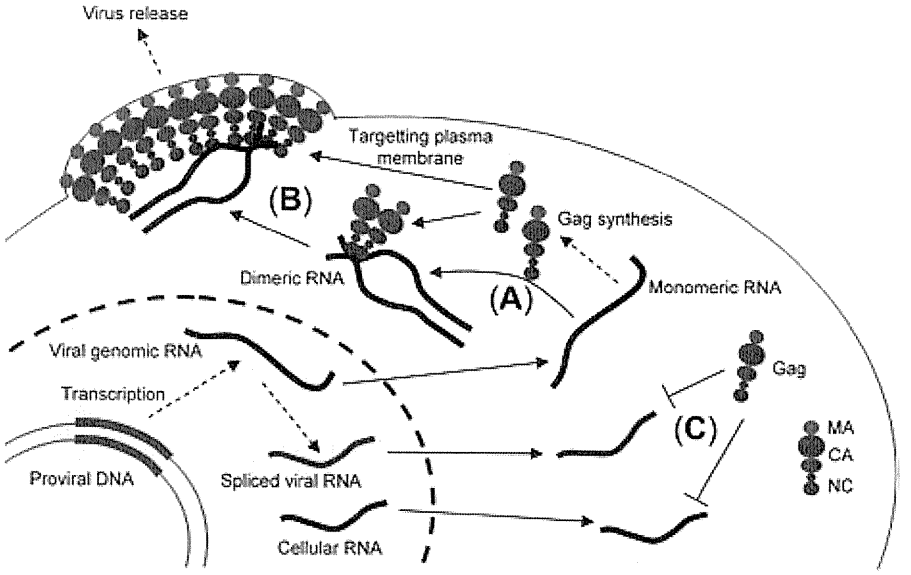

FIGURE 1 | Illustration showing retroviral genome packaging events. The retroviral genomic RNA is exported from the nucleus to cytoplasm and used as the mRNA for ribosomal synthesis of the Gag and Gag–Pol polyproteins. **(A)** The retroviral genomic RNA promotes conversion of the dimeric form of genomic RNA via the NC domain of Gag. **(B)** The Gag and retroviral genomic RNA complex is transported to the plasma membrane, where further assembly and budding occur, mediated by the myristoylated MA domain of Gag. **(C)** In contrast, spliced viral RNA or cellular RNA is not bound to the NC domain of Gag or may be bound to a small number of Gag polyproteins insufficient for trafficking to the plasma membrane.

MOLONEY MURINE LEUKEMIA VIRUS

Moloney murine leukemia virus is a simple prototypical retrovirus, with a single splicing event producing a spliced RNA for synthesizing Env during its life cycle. MoMLV is one of the most extensively studied retroviruses. Nucleotides 215–565 of the 5′ UTR have been identified as a responsible site for genome packaging (Ψ-site; Mann et al., 1983). The secondary structure of the 5′ UTR was determined by RNase protection assays using cross-linking reagents combined with computational analyses such as phylogenetic and free-energy calculations (Tounekti et al., 1992; Mougel et al., 1993). The monomeric Ψ-site is composed of a series of RNA stem-loops. Differences in RNase protection patterns were observed for the dimeric Ψ-site (Tounekti et al., 1992; Mougel et al., 1993; D'Souza and Summers, 2005). It was reported that a dimerized RNA fragment containing the entire Ψ-site was bound to a significant number of NCs (Miyazaki et al., 2010a). Meanwhile, a mutant RNA fragment that inhibited dimerization was bound to a few NCs. Thus, dimerization-dependent genome packaging is strongly indicated in MoMLV.

The minimum region sufficient for genome packaging is referred to as the core encapsidation signal (Ψ^{CES}), though a virus containing only Ψ^{CES} exhibits less efficient packaging than a virus containing the entire Ψ-site (Bender et al., 1987; Adam and Miller, 1988; Murphy and Goff, 1989; Mougel and Barklis, 1997; Yu et al., 2000). Ψ^{CES} consists of three RNA stem-loops (DIS-2, SL-C, and SL-D, see **Figures 2A,B**). DIS-2 harbors a palindromic sequence and is able to convert heterologous extended dimers. The structure of NC in a complex with a mutant RNA of Ψ^{CES} mimicking the dimer-like conformation was determined by nuclear magnetic resonance (NMR) spectroscopy (**Figures 2C,D**; D'Souza and Summers, 2004). UAUCUG residues sequestered by base-pairing in the monomeric conformation are exposed as a linker by dimerization. NC recognizes the UCUG sequence. NC is a highly basic protein, consisting of a zinc knuckle motif and labile tails in both the N- and C-terminus. Biophysical study indicated that NC specifically recognizes RNA fragments including a Py (C or U) – Py-Py-G sequence (Dey et al., 2005). The interface of NC–UCUG is complementary in both shape and charge (D'Souza and Summers, 2004; Dey et al., 2005). The guanosine base attaches to the deep hydrophobic pocket of the zinc knuckle via hydrophobic and hydrogen bonds. The three upstream nucleotides make contact with hydrophobic residues on the surface of the zinc knuckle.

SL-C and SL-D, which are part of Ψ^{CES}, promote genome packaging (Mougel et al., 1996; Mougel and Barklis, 1997; Fisher and Goff, 1998). Both are highly conserved among gammaretroviruses and contain GACG loops (Konings et al., 1992; Kim and Tinoco, 2000; D'Souza et al., 2001). A stem loop RNA fragment containing the GACG tetra-loop has a unique property (Kim and Tinoco, 2000). The C and G (3′) residues of the loop undergo intermolecular base-pairing (kissing interactions). This property of the stem loop containing GACG has led to speculation that SL-C and SL-D function in genome dimerization (Kim and Tinoco, 2000; D'Souza et al., 2001; Hibbert et al., 2004). Interestingly, the RNA fragment of SL-C forms two alternative conformations (one containing the GACG tetra-loop and the other, a CGAGU loop; Miyazaki et al., 2010b). NMR data showed that SL–CD was in a state of equilibrium between kissing and non-kissing interactions even at a high sample concentration and physiological ion-strength. The two alternative conformations of SL-C may regulate genome dimerization though the biological meaning of this is not yet clear.

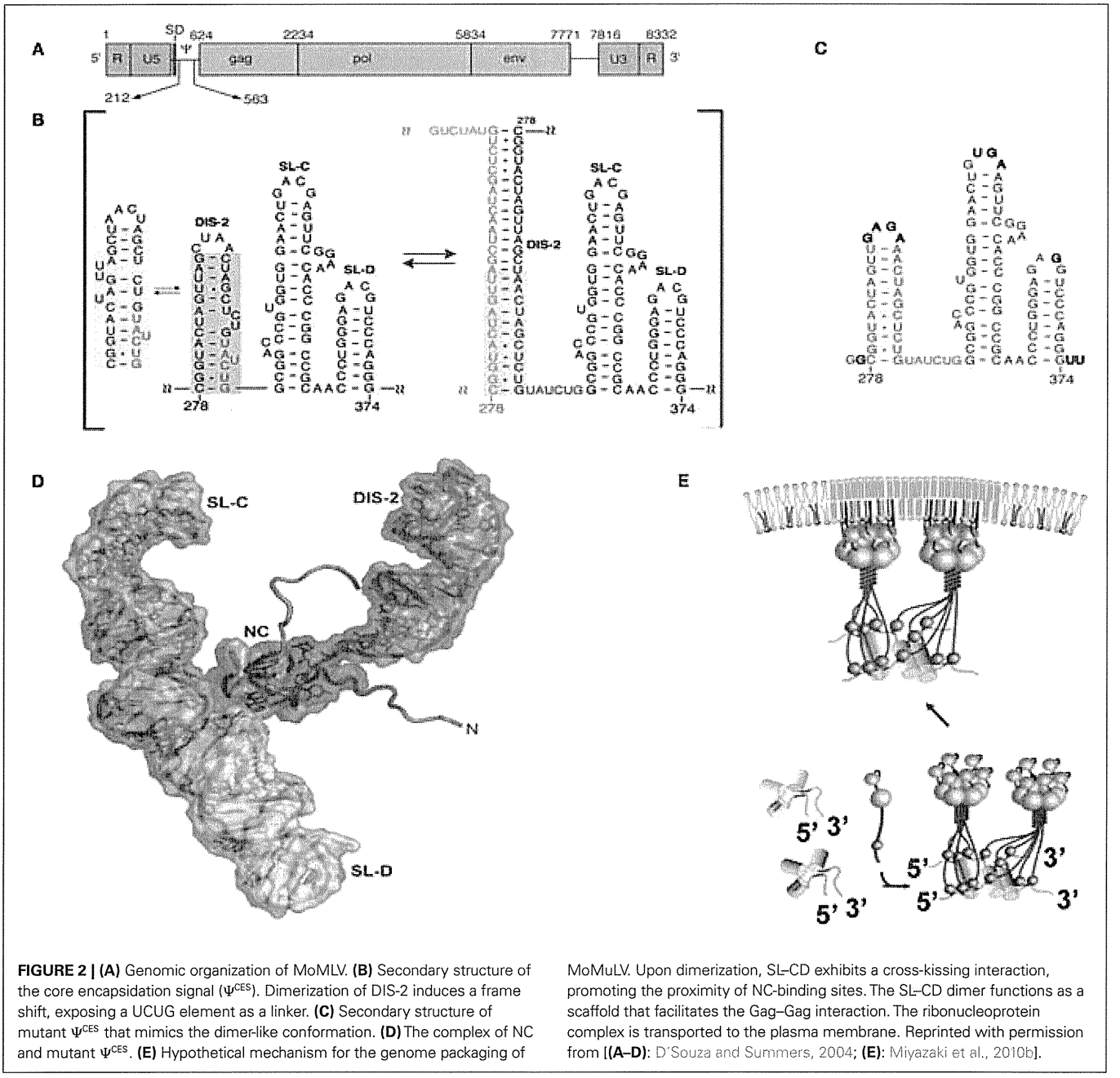

FIGURE 2 | (A) Genomic organization of MoMLV. **(B)** Secondary structure of the core encapsidation signal (Ψ^{CES}). Dimerization of DIS-2 induces a frame shift, exposing a UCUG element as a linker. **(C)** Secondary structure of mutant Ψ^{CES} that mimics the dimer-like conformation. **(D)** The complex of NC and mutant Ψ^{CES}. **(E)** Hypothetical mechanism for the genome packaging of MoMuLV. Upon dimerization, SL-CD exhibits a cross-kissing interaction, promoting the proximity of NC-binding sites. The SL-CD dimer functions as a scaffold that facilitates the Gag–Gag interaction. The ribonucleoprotein complex is transported to the plasma membrane. Reprinted with permission from [**(A–D)**: D'Souza and Summers, 2004; **(E)**: Miyazaki et al., 2010b].

The tertiary structure of a RNA fragment of a SL–CD mutant locking to form a single conformation containing the GACG terra-loop was determined by NMR spectroscopy and confirmed by Cryo-electron tomography (Miyazaki et al., 2010b). The structure revealed that SL–CD is dimerized by intermolecular cross-kissing (SL-C to SL-D′ and SL-D to SL-C′). These intermolecular cross-kissing interactions were also proposed based on selective 2′-Hydroxyl acylation analyzed by primer extension (SHAPE; Gherghe and Weeks, 2006; Gherghe et al., 2010). In addition, SL-C and SL-D stack end to end. Consequently, the two residues at the 5′-end of the SL–CD dimer are separated by ~20 Å. There are two UCUG sequences just upstream of SL-C. The intermolecular kissing interactions of SL-C and SL-D induce the proximity of four of the NC-binding sites. The genomic RNA has been suggested to promote the retroviral Gag/Gag interaction (Dawson and Yu, 1998; Burniston et al., 1999; Campbell and Rein, 1999; Cimarelli et al., 2000; Sandefur et al., 2000; Khorchid et al., 2002; Huseby et al., 2005). Both the DIS DIS-1 and DIS-2 are followed by two UCUG elements. The abundance and proximity of exposed UCUG and related elements within the dimeric 5′ UTR may facilitate Gag–Gag interactions (**Figure 2E**).

Of note, a totally different monomeric structure for a portion of the Ψ-site (nucleotides 205–374) was proposed based on SHAPE (Gherghe and Weeks, 2006), where the RNA region spanning nucleotides 231–315 forms a large stem-loop structure, which contains residues corresponding to DIS-2. SL-C also differed from

the structure previously reported, where the bottom of the stem is unstructured. It is suggested that the intermolecular kissing interactions of SL-C and SL-D induce the conformational change of SL-C and promote the dimerization of DIS-2. The difference in RNA structures may be due to the difference of RNA fragments used in those studies.

HUMAN IMMUNODEFICIENCY VIRUS TYPE 1

Virological studies have indicated the HIV-1 5′ leader region including the entire 5′ UTR and a portion of the *gag* coding region to be involved in genome packaging (Lever et al., 1989; Aldovini and Young, 1990; Clavel and Orenstein, 1990; Poznansky et al., 1991; Buchschacher and Panganiban, 1992; Kim et al., 1994; Luban and Goff, 1994; Parolin et al., 1994; Berkowitz et al., 1995; McBride and Panganiban, 1996, 1997; McBride et al., 1997; Harrison et al., 1998; Helga-Maria et al., 1999; Clever et al., 2002; Russell et al., 2002; Sakuragi et al., 2003, 2007). The 5′ leader RNA consists of a series of RNA stem-loops referred to as the transacting responsive element (TAR), primer-binding site (PBS), polyadenylation signal [poly(A)], DIS, SD, and residues spanning the *gag* start codon (AUG; **Figure 3**; Hayashi et al., 1992, 1993; Baudin et al., 1993; Skripkin et al., 1994; Clever et al., 1995; McBride and Panganiban, 1996, 1997; Clever and Parslow, 1997; Harrison et al., 1998; Damgaard et al., 2004; Wilkinson et al., 2008; Watts et al., 2009). It has been suggested that an RNA fragment of the 5′ leader RNA has two alternative conformations, whose secondary structure has been determined by chemical probing assays (Berkhout and van Wamel, 2000). One conformation is referred to as the long distance interaction (LDI) structure, in which the residues of DIS are base-paired with those of poly(A) and SD. The other conformation is referred to as the branched multiple hairpin structure (BMH), in which the residues of DIS, SD, and Ψ form a stem-loop structure as indicated before (Huthoff and Berkhout, 2001). In addition, the residues of AUG form base-pairs with the residues of the unique 5′ region (U5). Of note, it has been proposed a lot of secondary structural models for the 5′ leader (Lu et al., 2011b). NC catalyzes LDI to BMH. DIS is exposed as a stem-loop in BMH, which promotes the kissing dimer conformation and following the genome packaging event. However, the BMH structure is mostly observed in HIV-1-infected cells, but the LDI structure fails to be detected (Paillart et al., 2004a). Thus, the biological significance of the BMH/LDI riboswitch model remains to be elucidated.

RNA fragments of DIS, SD, Ψ, and AUG have been studied extensively since the region from DIS to AUG was initially identified as a Ψ-site (Lever et al., 1989; Aldovini and Young, 1990; Clavel and Orenstein, 1990; Poznansky et al., 1991; Harrison and Lever, 1992; Kim et al., 1994; McBride and Panganiban, 1996, 1997; Harrison et al., 1998). The RNA fragments of SD and Ψ are bound to NC with high affinity (Clever et al., 1995; Amarasinghe et al., 2000a,b), whereas the RNA fragments of DIS and AUG are bound to NC with relatively low affinity (Darlix et al., 1990; Amarasinghe et al., 2001; Lawrence et al., 2003). The RNA fragment of Ψ is bound to NC with the highest affinity ($K_d = 100$ nM) among these four RNA fragments (Amarasinghe et al., 2000b). Deletion or destabilization of the stem of Ψ results in a significant reduction in genome packaging efficiency (Clever and Parslow, 1997; McBride and Panganiban, 1997). This indicates that the stem-loop

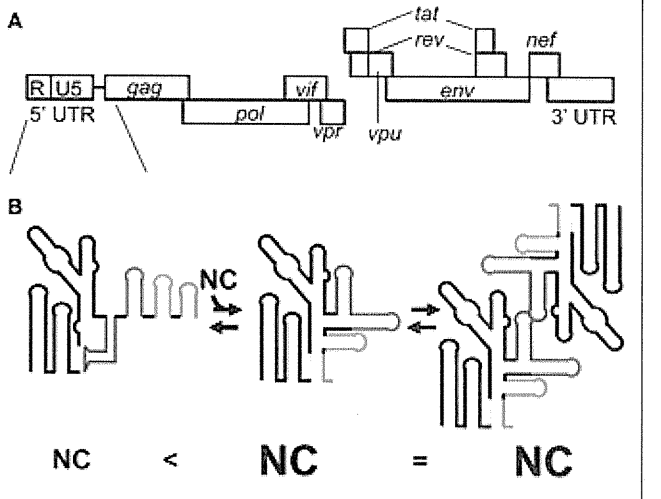

FIGURE 3 | (A) Genomic organization of HIV-1. **(B)** The latest model for HIV-1 genome packaging. Conformational change of RNA in the 5′ leader region regulates genome dimerization and genome packaging. The stem-loop structure of AUG causes sequestering of DIS via long range interaction with the residues of U5, resulting in the inhibition of HIV-1 genome dimerization (left). In this conformation of the 5′ leader RNA, a small number of NCs are capable of binding the 5′ leader RNA. In contrast, the interaction of AUG with U5 residues promotes genome dimerization via exposure of DIS (center). In this conformation of the 5′ leader RNA, a greater number of NCs are capable of binding the 5′ leader RNA. The different RNA elements in the 5′ leader region are color coded: DIS (red), SD (blue), Ψ (orange), and AUG (green).

structure of Ψ is important for genome packaging. Ψ consists of a GGAG tetra-loop and a stem. The structure of the ribonucleoprotein complex NC–Ψ has been determined by NMR spectroscopy. Guanosine residues of the GGAG tetra-loop are inserted into the hydrophobic clefts of both the N- and C-terminal zinc knuckles (De Guzman et al., 1998). The adenosine residue of the loop packs against the N-terminal zinc knuckle and an N-terminal alpha-helix domain binds to the major groove of the RNA stem. Thus, overall, NC residues are involved in binding with Ψ RNA, by which the tight binding of NC–Ψ is achieved. In addition, the intramolecular interaction of two zinc knuckles may help to stabilize the complex of NC and Ψ RNA.

The RNA fragment of SD is also bound to NC with high affinity though the binding is slightly weaker than that of Ψ (Amarasinghe et al., 2000a). SD RNA contains a GGUG tetra-loop and a stem containing a characteristic AUA triple base-pairing structure. All guanosine residues of the loop inserted into the hydrophobic clefts of zinc knuckles as observed in the complex of NC and Ψ RNA. A major structural difference between the NC and SD RNA complex and the NC and Ψ RNA complex is the orientation of the N-terminal alpha-helix domain of NC. The domain does not stick into SD RNA and is exposed outside of SD RNA. The N-terminal zinc knuckle interacts with an AUA triple base-pairing motif in the minor groove of the SD RNA stem. A mutant virus with a disrupted lower stem structure of SD exhibited a 20% reduction in genome packaging compared with the wild-type virus, despite the robust binding of Ψ RNA and NC (McBride and Panganiban,

1997). Further study will be needed to clarify the link between the tight binding of SD RNA with NC and its biological relevance.

Dimer initiation site contains a GC-rich palindromic sequence and an inner bulge (G-AGG) in the middle of the stem. This inner bulge is recognized by NC. As described above, guanosine residues not in base-pairs possibly play an important role in the binding to NC (Mihailescu and Marino, 2004). However, the binding affinity of NC–DIS is relatively weak (approximately five times weaker than that of NC–SD/ Ψ; Lawrence et al., 2003). NC catalyzes the conversion of DIS from a kissing dimer to a more stable extended duplex conformation (Darlix et al., 1990; Feng et al., 1996). Virological studies have suggested that interaction between the two 5′ UTR is required for genome packaging (Sakuragi et al., 2001, 2002). A very recent study indicated that genome dimerization is controlled by a unique strategy (**Figure 3B**). RNA containing the entire 5′ UTR and the first 21 residues of the *gag* coding region forms two alternative conformations (Lu et al., 2011a). In one conformation, DIS is sequestered via a long range interaction with U5, which inhibits genome dimerization. In the other conformation, DIS is exposed by release from the interaction with U5, which promotes genome dimerization.

AUG was believed to form a stem-loop structure, consisting of a GAGA tetra-loop and an unstable short stem containing two wobble G–U base-pairs (Amarasinghe et al., 2001). The GAGA tetra-loop is a type of GNRA (N is A, C, G, or U; R is A or G) tetra-loop, which is frequently observed in ribosomal RNA. GNRA tetra-loop helps fold stem-loops, and one Watson–Crick base-pair is enough to close off the RNA fragment. However, it has been suggested that AUG does not form a stem-loop structure and a portion of the residues of AUG may have a long range interaction with the residues of U5 as indicated in the BMH structure (Abbink and Berkhout, 2003; Damgaard et al., 2004; Spriggs et al., 2008; Wilkinson et al., 2008; Watts et al., 2009). Studies using deletion mutants indicate that the entire 5′ UTR and *gag* coding regions are important for genome packaging (Buchschacher and Panganiban, 1992; Luban and Goff, 1994; Parolin et al., 1994; Clever et al., 2002; Russell et al., 2002). Evidence of the importance of long range interactions for genome packaging was reported recently (**Figure 3B**; Lu et al., 2011a). It shows that AUG regulates genome dimerization. AUG forms two alternative conformations. One is a stem-loop conformation as initially suggested. The other is a complex with the residues of U5. The interaction of AUG with U5 leads to the exposure of DIS, promoting genome dimerization. Of note, when the residues of AUG form a stem-loop structure, in which the dimerization of the 5′ leader RNA is inhibited, a small number of NCs can bind the 5′ leader RNA (**Figure 3B**). On the other hand, when the residues of AUG interact with the residues of U5, a greater number of NCs can bind the 5′ leader RNA. Thus, AUG has a critical role in genome dimerization and genome packaging. In addition, it is suggested that the residues ranging from the end of Ψ to the start of AUG form base-pairing with the residues of the 3′ terminus of PBS. That is also proposed by earlier work Lu et al. (2011b). In fact, Sakuragi et al. (2003, 2007) indicate these residues are indispensable both for genome dimerization and genome packaging *in vivo*.

It is suggested that the HIV-1 genome's dimerization and packaging are controlled by dynamic changes of the 5′ leader's conformation as indicated in MoMLV (D'Souza and Summers, 2004; Miyazaki et al., 2010a; Lu et al., 2011a). Ψ is indicated to be important for genome packaging, however, it is not clear how Ψ works in the model suggested by Lu et al. (2011a). This will be the next question to answer for a better understanding of the molecular mechanism of HIV-1 genome packaging.

HUMAN IMMUNODEFICIENCY VIRUS TYPE 2

Human immunodeficiency virus type 2 (HIV-2) is one of two human lentiviruses that can cause AIDS. HIV-1 and HIV-2 exhibit approximately 55% nucleotide sequence identity. However, they differ significantly in their 5′ UTR. For example, the 5′ UTR of HIV-2 (HIV-2_{ROD}) consists of 535 nucleotides, whereas that of HIV-1 (HIV-1_{NL432}) consists of 335 nucleotides. The 5′ leader RNA of HIV-2 contains three unique RNA elements referred to as Ψ-1, Ψ-2, and Ψ-3 in addition to a series of RNA stem-loops, TAR, poly(A), PBS, DIS, SD, and AUG, those are commonly observed in the 5′ leader of HIV-1 (**Figure 4**; Berkhout, 1996). The structure of HIV-2 NC also exhibits some different features. A major difference in NC between HIV-2 and HIV-1 is the structure of the N-terminal flanking domain (Berkhout, 1996; Jewell and Mansky, 2000; Matsui et al., 2009). The N-terminal domain of HIV-1 NC forms an alpha-helix, whereas that of HIV-2 NC is too short to do so. Another difference is the intra-molecular interaction of two zinc knuckles of HIV-2 NC, by which HIV-2 NC forms a more globular structure than HIV-1 NC. These structural differences of NCs between HIV-1 and HIV-2 may affect RNA recognition.

It has been suggested that Ψ-3 can be bound to NC (Tsukahara et al., 1996; Damgaard et al., 1998). A study using RNase protection assays suggested that the NC–Ψ-3 ribonucleoprotein exhibited strong protection at the loop of Ψ-3. This was supported by NMR experiments. The guanosine residue of the UUAGAC loop is inserted into the hydrophobic cleft of the C-terminal zinc knuckle (Matsui et al., 2009). The N-terminal zinc knuckle does not bind the RNA fragment of Ψ-3. However, virological study has suggested that Ψ-3 is not essential for either genome dimerization or genome packaging (McCann and Lever, 1997). In agreement with that, a recent study showed that NC binds the RNA fragment of Ψ-3 with 100 times lower affinity than HIV-1 NC binds the RNA fragment of HIV-1 Ψ (Purzycka et al., 2011).

The RNA fragment of DIS is bound to NC with high affinity ($K_d = 100$ nM), equivalent to the affinity of HIV-1 Ψ RNA and the cognate NC (Purzycka et al., 2011). HIV-2 NC recognizes the inner bulge of DIS, and does not bind to the loop. HIV-1 DIS is weakly bound to the cognate NC (Lawrence et al., 2003; Andersen et al., 2004). Interestingly, HIV-2 TAR and poly(A) is bound to the NCs with relatively high affinity (TAR–NC Kd = 450 nM, poly(A) – NC Kd = 550 nM). All the tight NC-binding sites [DIS, TAR, and poly(A)] are located upstream of SD. The regions responsible for the genome packaging of retroviruses are generally located downstream of SD, by which the genomic RNA is selectively packaged from an excess amount of spliced viral RNA. It is suggested that HIV-2 genome packaging is primarily mediated by *cis* packaging mechanism (Kaye and Lever, 1999; Griffin et al., 2001; L'Hernault et al., 2007). The Gag packages genomic RNA from which it is translated. Therefore, the HIV-2 Gag is not required to distinguish the genomic RNA from viral spliced RNAs. Recent

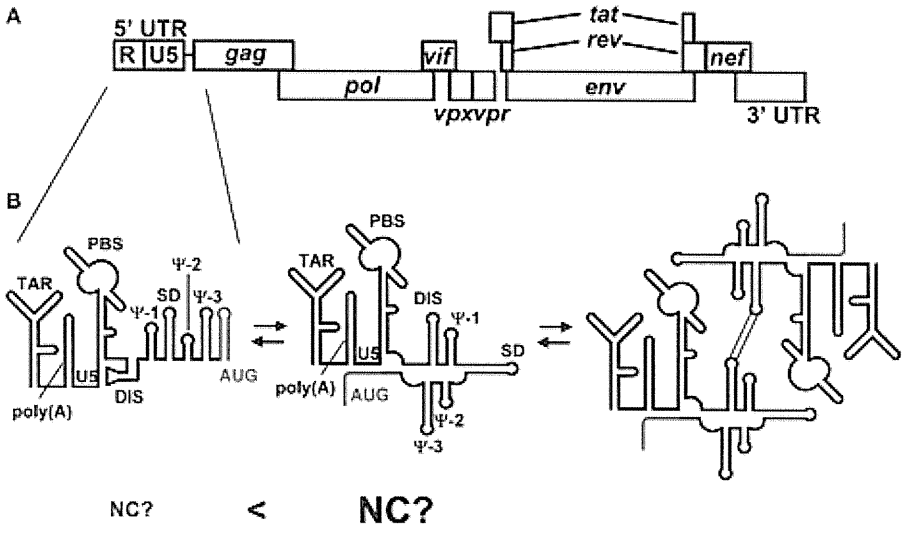

FIGURE 4 | (A) Genomic organization of HIV-2. **(B)** Representative secondary structures predicted for the 5′ UTR of HIV-2. Variations among recent predictions for AUG (green) are shown. The residues of AUG have been suggested to form a stem-loop structure and show long range interaction with the residues of U5. It has been suggested that HIV-2 genome's dimerization is employed the same mechanism as HIV-1. However, it remains to be clear whether NC preferentially binds the 5′ leader RNA containing the U5–AUG interaction.

studies, however, indicated that HIV-2 genome packaging is primarily mediated by *trans* packaging mechanism (Ni et al., 2011). TAR contains a palindromic sequence and has been suggested to form a dimer (Berkhout et al., 1993; Andersen et al., 2004). The dimerization of TAR may also function for efficient genome packaging. Further study will be needed to determine how the RNA elements located upstream of SD are involved in genome packaging.

Despite significant differences in the recognition of NC by the 5′ leader RNA, HIV-1, and HIV-2 may employ similar mechanisms for genome packaging. Dirac et al. (2002) observed that the RNA fragment of the 5′ leader region forms two alternative conformations as observed for the HIV-1 RNA fragments of the 5′ leader region. The long range interaction of U5–AUG is observed for the BMH conformation though it is not clear whether the LDI/BMH riboswitch mechanism is utilized for genome packaging *in vivo*. Recent study also indicated the U5–AUG interaction by SHAPE analysis (Purzycka et al., 2011). Of note, it is suggested that the U5–AUG interaction regulates the HIV-2 genome dimerization as indicated in HIV-1 (Baig et al., 2008). Lu et al. (2011a) suggest that the 5′ leader RNA containing the U5–AUG interaction of HIV-1 is preferentially bound to the cognate NC. A major question is whether the U5–AUG interaction of HIV-2 also promotes the NC-binding to the 5′ leader RNA (**Figure 4B**). Phylogenetic and computational analyses suggested that the U5–AUG long range interaction is widely conserved among retroviruses (Damgaard et al., 2004). The long range interaction of U5–AUG may be important for retroviral genome dimerization and genome packaging.

PERSPECTIVES

It has been indicated that the MoMLV NC domain of Gag binds predominantly to dimeric genomes (D'Souza and Summers, 2004; Miyazaki et al., 2010a). HIV-1 was indicated to have a similar system (Lu et al., 2011a). MoMLV showed proximal NC-binding motifs in Ψ^{CES}, implying that Gag–Gag multimerization is initiated by genomic RNA (Miyazaki et al., 2010b). A major question is whether the proximity of NC-binding motifs is observed for other retroviruses such as HIV-1 and HIV-2. In addition, is the proximity of NC-binding motifs essential for retroviral genome packaging? Further study for these questions will lead to a better understanding for the molecular mechanism underlying retroviral genome packaging.

ACKNOWLEDGMENTS

This work was supported in part by a Grant-in-Aid for Scientific Research (B) from the Japan Society for the Promotion of Science (ID no. 21390141).

REFERENCES

Abbink, T. E. M., and Berkhout, B. (2003). A novel long distance base-pairing interaction in human immunodeficiency virus type 1 RNA occludes the Gag start codon. *J. Biol. Chem.* 278, 11601–11611.

Adam, M. A., and Miller, A. D. (1988). Identification of a signal in a murine retrovirus that is sufficient for packaging of nonretroviral RNA into virions. *J. Virol.* 62, 3802–3806.

Aldovini, A., and Young, R. A. (1990). Mutations of RNA and protein sequences involved in human immunodeficiency virus type 1 packaging result in production of noninfectious virus. *J. Virol.* 64, 1920–1926.

Amarasinghe, G. K., De Guzman, R. N., Turner, R. B., Chancellor, K. J., Wu, Z. R., and Summers, M. F. (2000a). NMR structure of the HIV-1 nucleocapsid protein bound to stem-loop SL2 of the psi-RNA packaging signal. Implications for genome recognition. *J. Mol. Biol.* 301, 491–511.

Amarasinghe, G. K., De Guzman, R. N., Turner, R. B., and Summers, M. F. (2000b). NMR structure of stem-loop SL2 of the HIV-1 psi RNA packaging signal reveals a novel A-U-A base-triple platform. *J. Mol. Biol.* 299, 145–156.

Amarasinghe, G. K., Zhou, J., Miskimon, M., Chancellor, K. J., McDonald, J. A., Matthews, A. G., Miller, R. R., Rouse, M. D., and Summers, M. F. (2001). Stem-loop SL4 of the HIV-1 psi RNA packaging signal exhibits weak affinity for the nucleocapsid protein. Structural studies and implications for genome recognition. *J. Mol. Biol.* 314, 961–970.

Andersen, E. S., Contera, S. A., Knudsen, B., Damgaard, C. K., Besenbacher, F., and Kjems, J. (2004). Role of the trans-activation response element in dimerization of HIV-1 RNA. *J. Biol. Chem.* 279, 22243–22249.

Baig, T. T., Strong, C. L., Lodmell, J. S., and Lanchy, J. M. (2008). Regulation of primate lentiviral RNA dimerization by structural entrapment. *Retrovirology* 5, 65.

Baudin, F., Marquet, R., Isel, C., Darlix, J. L., Ehresmann, B., and Ehresmann, C. (1993). Functional sites in the 5′ region of human immunodeficiency virus type 1 RNA form defined structural domains. *J. Mol. Biol.* 229, 382–397.

Bender, M. A., Palmer, T. D., Gelinas, R. E., and Miller, A. D. (1987). Evidence that the packaging signal of Moloney murine leukemia virus extends into the gag region. *J. Virol.* 61, 1639–1646.

Berkhout, B. (1996). Structure and function of the human immunodeficiency virus leader RNA. *Prog. Nucleic Acid Res. Mol. Biol.* 54, 1–34.

Berkhout, B., Essink, B. B., and Schoneveld, I. (1993). In vitro dimerization of HIV-2 leader RNA in the absence of PuGGAPuA motifs. *FASEB J.* 7, 181–187.

Berkhout, B., and van Wamel, J. L. (2000). The leader of the HIV-1 RNA genome forms a compactly folded tertiary structure. *RNA* 6, 282–295.

Berkowitz, R., Fisher, J., and Goff, S. P. (1996). RNA packaging. *Curr. Top. Microbiol. Immunol.* 214, 177–218.

Berkowitz, R. D., Hammarskjöld, M. L., Helga-Maria, C., Rekosh, D., and Goff, S. P. (1995). 5′ Regions of HIV-1 RNAs are not sufficient for encapsidation: implications for the HIV-1 packaging signal. *Virology* 212, 718–723.

Browning, M. T., Mustafa, F., Schmidt, R. D., Lew, K. A., and Rizvi, T. A. (2003). Delineation of sequences important for efficient packaging of feline immunodeficiency virus RNA. *J. Gen. Virol.* 84, 621–627.

Buchschacher, G. L., and Panganiban, A. T. (1992). Human immunodeficiency virus vectors for inducible expression of foreign genes. *J. Virol.* 66, 2731–2739.

Burniston, M. T., Cimarelli, A., Colgan, J., Curtis, S. P., and Luban, J. (1999). Human immunodeficiency virus type 1 Gag polyprotein multimerization requires the nucleocapsid domain and RNA and is promoted by the capsid-dimer interface and the basic region of matrix protein. *J. Virol.* 73, 8527–8540.

Campbell, S., and Rein, A. (1999). In vitro assembly properties of human immunodeficiency virus type 1 Gag protein lacking the p6 domain. *J. Virol.* 73, 2270–2279.

Cimarelli, A., Sandin, S., Höglund, S., and Luban, J. (2000). Basic residues in human immunodeficiency virus type 1 nucleocapsid promote virion assembly via interaction with RNA. *J. Virol.* 74, 3046–3057.

Clavel, F., and Orenstein, J. M. (1990). A mutant of human immunodeficiency virus with reduced RNA packaging and abnormal particle morphology. *J. Virol.* 64, 5230–5234.

Clever, J., Sassetti, C., and Parslow, T. G. (1995). RNA secondary structure and binding sites for gag gene products in the 5′ packaging signal of human immunodeficiency virus type 1. *J. Virol.* 69, 2101–2109.

Clever, J. L., Miranda, D., and Parslow, T. G. (2002). RNA structure and packaging signals in the 5′ leader region of the human immunodeficiency virus type 1 genome. *J. Virol.* 76, 12381–12387.

Clever, J. L., and Parslow, T. G. (1997). Mutant human immunodeficiency virus type 1 genomes with defects in RNA dimerization or encapsidation. *J. Virol.* 71, 3407–3414.

Damgaard, C. K., Andersen, E. S., Knudsen, B., Gorodkin, J., and Kjems, J. (2004). RNA interactions in the 5′ region of the HIV-1 genome. *J. Mol. Biol.* 336, 369–379.

Damgaard, C. K., Dyhr-Mikkelsen, H., and Kjems, J. (1998). Mapping the RNA binding sites for human immunodeficiency virus type-1 gag and NC proteins within the complete HIV-1 and -2 untranslated leader regions. *Nucleic Acids Res.* 26, 3667–3676.

Darlix, J. L., Gabus, C., Nugeyre, M. T., Clavel, F., and Barré-Sinoussi, F. (1990). *Cis* elements and trans-acting factors involved in the RNA dimerization of the human immunodeficiency virus HIV-1. *J. Mol. Biol.* 216, 689–699.

Dawson, L., and Yu, X. F. (1998). The role of nucleocapsid of HIV-1 in virus assembly. *Virology* 251, 141–157.

De Guzman, R. N., Wu, Z. R., Stalling, C. C., Pappalardo, L., Borer, P. N., and Summers, M. F. (1998). Structure of the HIV-1 nucleocapsid protein bound to the SL3 psi-RNA recognition element. *Science* 279, 384–388.

Dey, A., York, D., Smalls-Mantey, A., and Summers, M. F. (2005). Composition and sequence-dependent binding of RNA to the nucleocapsid protein of Moloney murine leukemia virus. *Biochemistry* 44, 3735–3744.

Dirac, A. M. G., Huthoff, H., Kjems, J., and Berkhout, B. (2002). Regulated HIV-2 RNA dimerization by means of alternative RNA conformations. *Nucleic Acids Res.* 30, 2647–2655.

D'Souza, V., Melamed, J., Habib, D., Pullen, K., Wallace, K., and Summers, M. F. (2001). Identification of a high affinity nucleocapsid protein binding element within the Moloney murine leukemia virus Psi-RNA packaging signal: implications for genome recognition. *J. Mol. Biol.* 314, 217–232.

D'Souza, V., and Summers, M. F. (2004). Structural basis for packaging the dimeric genome of Moloney murine leukaemia virus. *Nature* 431, 586–590.

D'Souza, V., and Summers, M. F. (2005). How retroviruses select their genomes. *Nat. Rev. Microbiol.* 3, 643–655.

Feng, Y. X., Copeland, T. D., Henderson, L. E., Gorelick, R. J., Bosche, W. J., Levin, J. G., and Rein, A. (1996). HIV-1 nucleocapsid protein induces "maturation" of dimeric retroviral RNA in vitro. *Proc. Natl. Acad. Sci. U.S.A.* 93, 7577–7581.

Fisher, J., and Goff, S. P. (1998). Mutational analysis of stem-loops in the RNA packaging signal of the Moloney murine leukemia virus. *Virology* 244, 133–145.

Gherghe, C., Leonard, C. W., Gorelick, R. J., and Weeks, K. M. (2010). Secondary structure of the mature ex virio Moloney murine leukemia virus genomic RNA dimerization domain. *J. Virol.* 84, 898–906.

Gherghe, C., and Weeks, K. M. (2006). The SL1-SL2 (stem-loop) domain is the primary determinant for stability of the gamma retroviral genomic RNA dimer. *J. Biol. Chem.* 281, 37952–37961.

Greatorex, J. (2004). The retroviral RNA dimer linkage: different structures may reflect different roles. *Retrovirology* 1, 22.

Griffin, S. D., Allen, J. F., and Lever, A. M. (2001). The major human immunodeficiency virus type 2 (HIV-2) packaging signal is present on all HIV-2 RNA species: cotranslational RNA encapsidation and limitation of Gag protein confer specificity. *J. Virol.* 75, 12058–12069.

Harrison, G. P., and Lever, A. M. (1992). The human immunodeficiency virus type 1 packaging signal and major splice donor region have a conserved stable secondary structure. *J. Virol.* 66, 4144–4153.

Harrison, G. P., Miele, G., Hunter, E., and Lever, A. M. (1998). Functional analysis of the core human immunodeficiency virus type 1 packaging signal in a permissive cell line. *J. Virol.* 72, 5886–5896.

Hayashi, T., Shioda, T., Iwakura, Y., and Shibuta, H. (1992). RNA packaging signal of human immunodeficiency virus type 1. *Virology* 188, 590–599.

Hayashi, T., Ueno, Y., and Okamoto, T. (1993). Elucidation of a conserved RNA stem-loop structure in the packaging signal of human immunodeficiency virus type 1. *FEBS Lett.* 327, 213–218.

Helga-Maria, C., Hammarskjöld, M. L., and Rekosh, D. (1999). An intact TAR element and cytoplasmic localization are necessary for efficient packaging of human immunodeficiency virus type 1 genomic RNA. *J. Virol.* 73, 4127–4135.

Henderson, L. E., Copeland, T. D., Sowder, R. C., Smythers, G. W., and Oroszlan, S. (1981). Primary structure of the low molecular weight nucleic acid-binding proteins of murine leukemia viruses. *J. Biol. Chem.* 256, 8400–8406.

Hibbert, C. S., Mirro, J., and Rein, A. (2004). mRNA molecules containing murine leukemia virus packaging signals are encapsidated as dimers. *J. Virol.* 78, 10927–10938.

Huseby, D., Barklis, R. L., Alfadhli, A., and Barklis, E. (2005). Assembly of human immunodeficiency virus precursor gag proteins. *J. Biol. Chem.* 280, 17664–17670.

Huthoff, H., and Berkhout, B. (2001). Two alternating structures of the HIV-1 leader RNA. *RNA* 7, 143–157.

Jewell, N. A., and Mansky, L. M. (2000). In the beginning: genome recognition, RNA encapsidation and the initiation of complex retrovirus assembly. *J. Gen. Virol.* 81, 1889–1899.

Kaye, J. F., and Lever, A. M. (1999). Human immunodeficiency virus types 1 and 2 differ in the predominant mechanism used for selection of genomic RNA for encapsidation. *J. Virol.* 73, 3023–3031.

Khorchid, A., Halwani, R., Wainberg, M. A., and Kleiman, L. (2002). Role of RNA in facilitating Gag/Gag-Pol interaction. *J. Virol.* 76, 4131–4137.

Kim, C. H., and Tinoco, I. (2000). A retroviral RNA kissing complex containing only two GC base pairs. *Proc. Natl. Acad. Sci. U.S.A.* 97, 9396–9401.

Kim, H. J., Lee, K., and O'Rear, J. J. (1994). A short sequence upstream of the 5′ major splice site is important for encapsidation of HIV-1 genomic RNA. *Virology* 198, 336–340.

Kodera, Y., Sato, K., Tsukahara, T., Komatsu, H., Maeda, T., and Kohno, T. (1998). High-resolution solution NMR structure of the minimal active domain of the human immunodeficiency virus type-2 nucleocapsid protein. *Biochemistry* 37, 17704–17713.

Konings, D. A., Nash, M. A., Maizel, J. V., and Arlinghaus, R. B. (1992). Novel GACG-hairpin pair motif in the 5′ untranslated region of type C retroviruses related to murine leukemia virus. *J. Virol.* 66, 632–640.

Laughrea, M., Jetté, L., Mak, J., Kleiman, L., Liang, C., and Wainberg, M. A. (1997). Mutations in the kissing-loop hairpin of human immunodeficiency virus type 1 reduce viral infectivity as well as genomic RNA packaging and dimerization. *J. Virol.* 71, 3397–3406.

Lawrence, D. C., Stover, C. C., Noznitsky, J., Wu, Z., and Summers, M. F. (2003). Structure of the intact stem and bulge of HIV-1 Psi-RNA stem-loop SL1. *J. Mol. Biol.* 326, 529–542.

Lever, A., Gottlinger, H., Haseltine, W., and Sodroski, J. (1989). Identification of a sequence required for efficient packaging of human immunodeficiency virus type 1 RNA into virions. *J. Virol.* 63, 4085–4087.

L'Hernault, A., Greatorex, J. S., Crowther, R. A., and Lever, A. M. L. (2007). Dimerisation of HIV-2 genomic RNA is linked to efficient RNA packaging, normal particle maturation and viral infectivity. *Retrovirology* 4, 90.

Lu, K., Heng, X., Garyu, L., Monti, S., Garcia, E. L., Kharytonchyk, S., Dorjsuren, B., Kulandaivel, G., Jones, S., Hiremath, A., Divakaruni, S. S., LaCotti, C., Barton, S., Tummillo, D., Hosic, A., Edme, K., Albrecht, S., Telesnitsky, A., and Summers, M. F. (2011a). NMR detection of structures in the HIV-1 5 ′-leader RNA that regulate genome packaging. *Science* 334, 242–245.

Lu, K., Heng, X., and Summers, M. F. (2011b). Structural determinants and mechanism of HIV-1 genome packaging. *J. Mol. Biol.* 410, 609–633.

Luban, J., and Goff, S. P. (1994). Mutational analysis of *cis*-acting packaging signals in human immunodeficiency virus type 1 RNA. *J. Virol.* 68, 3784–3793.

Mann, R., and Baltimore, D. (1985). Varying the position of a retrovirus packaging sequence results in the encapsidation of both unspliced and spliced RNAs. *J. Virol.* 54, 401–407.

Mann, R., Mulligan, R. C., and Baltimore, D. (1983). Construction of a retrovirus packaging mutant and its use to produce helper-free defective retrovirus. *Cell* 33, 153–159.

Mansky, L. M., Krueger, A. E., and Temin, H. M. (1995). The bovine leukemia virus encapsidation signal is discontinuous and extends into the 5′ end of the gag gene. *J. Virol.* 69, 3282–3289.

Matsui, T., Kodera, Y., Miyauchi, E., Tanaka, H., Endoh, H., Komatsu, H., Tanaka, T., Kohno, T., and Maeda, T. (2007). Structural role of the secondary active domain of HIV-2 NCp8 in multi-functionality. *Biochem. Biophys. Res. Commun.* 358, 673–678.

Matsui, T., Tanaka, T., Endoh, H., Sato, K., Tanaka, H., Miyauchi, E., Kawashima, Y., Nagai-Makabe, M., Komatsu, H., Kohno, T., Maeda, T., and Kodera, Y. (2009). The RNA recognition mechanism of human immunodeficiency virus (HIV) type 2 NCp8 is different from that of HIV-1 NCp7. *Biochemistry* 48, 4314–4323.

McBride, M. S., and Panganiban, A. T. (1996). The human immunodeficiency virus type 1 encapsidation site is a multipartite RNA element composed of functional hairpin structures. *J. Virol.* 70, 2963–2973.

McBride, M. S., and Panganiban, A. T. (1997). Position dependence of functional hairpins important for human immunodeficiency virus type 1 RNA encapsidation in vivo. *J. Virol.* 71, 2050–2058.

McBride, M. S., Schwartz, M. D., and Panganiban, A. T. (1997). Efficient encapsidation of human immunodeficiency virus type 1 vectors and further characterization of *cis* elements required for encapsidation. *J. Virol.* 71, 4544–5454.

McCann, E. M., and Lever, A. M. (1997). Location of *cis*-acting signals important for RNA encapsidation in the leader sequence of human immunodeficiency virus type 2. *J. Virol.* 71, 4133–41337.

Mihailescu, M. -R., and Marino, J. P. (2004). A proton-coupled dynamic conformational switch in the HIV-1 dimerization initiation site kissing complex. *Proc. Natl. Acad. Sci. U.S.A.* 101, 1189–1194.

Miyazaki, Y., Garcia, E. L., King, S. R., Iyalla, K., Loeliger, K., Starck, P., Syed, S., Telesnitsky, A., and Summers, M. F. (2010a). An RNA structural switch regulates diploid genome packaging by Moloney murine leukemia virus. *J. Mol. Biol.* 396, 141–152.

Miyazaki, Y., Irobalieva, R. N., Tolbert, B. S., Smalls-Mantey, A., Iyalla, K., Loeliger, K., D'Souza, V., Khant, H., Schmid, M. F., Garcia, E. L., Telesnitsky, A., Chiu, W., and Summers, M. F. (2010b). Structure of a conserved retroviral RNA packaging element by NMR spectroscopy and cryo-electron tomography. *J. Mol. Biol.* 404, 751–772.

Mougel, M., and Barklis, E. (1997). A role for two hairpin structures as a core RNA encapsidation signal in murine leukemia virus virions. *J. Virol.* 71, 8061–8065.

Mougel, M., Tounekti, N., Darlix, J. L., Paoletti, J., Ehresmann, B., and Ehresmann, C. (1993). Conformational analysis of the 5′ leader and the gag initiation site of Mo-MuLV RNA and allosteric transitions induced by dimerization. *Nucleic Acids Res.* 21, 4677–4684.

Mougel, M., Zhang, Y., and Barklis, E. (1996). *cis*-active structural motifs involved in specific encapsidation of Moloney murine leukemia virus RNA. *J. Virol.* 70, 5043–5050.

Murphy, J. E., and Goff, S. P. (1989). Construction and analysis of deletion mutations in the U5 region of Moloney murine leukemia virus: effects on RNA packaging and reverse transcription. *J. Virol.* 63, 319–327.

Mustafa, F., Lew, K. A., Schmidt, R. D., Browning, M. T., and Rizvi, T. A. (2004). Mutational analysis of the predicted secondary RNA structure of the Mason-Pfizer monkey virus packaging signal. *Virus Res.* 99, 35–46.

Nelson, P. N., Carnegie, P. R., Martin, J., Davari Ejtehadi, H., Hooley, P., Roden, D., Rowland-Jones, S., Warren, P., Astley, J., and Murray, P. G. (2003). Demystified. Human endogenous retroviruses. *Mol. Pathol.* 56, 11–18.

Ni, N., Nikolaitchik, O. A., Dilley, K. A., Chen, J., Galli, A., Fu, W., Prasad, V. V. S. P., Ptak, R. G., Pathak, V. K., and Hu, W. S. (2011). Mechanisms of human immunodeficiency virus type 2 RNA packaging: efficient *trans* packaging and selection of RNA copackaging partners. *J. Virol.* 85, 7603–7612.

Paillart, J. C., Dettenhofer, M., Yu, X. -F., Ehresmann, C., Ehresmann, B., and Marquet, R. (2004a). First snapshots of the HIV-1 RNA structure in infected cells and in virions. *J. Biol. Chem.* 279, 48397–48403.

Paillart, J. C., Shehu-Xhilaga, M., Marquet, R., and Mak, J. (2004b). Dimerization of retroviral RNA genomes: an inseparable pair. *Nat. Rev. Microbiol.* 2, 461–472.

Paillart, J. C., Marquet, R., Skripkin, E., Ehresmann, C., and Ehresmann, B. (1996). Dimerization of retroviral genomic RNAs: structural and functional implications. *Biochimie* 78, 639–653.

Parolin, C., Dorfman, T., Palú, G., Göttlinger, H., and Sodroski, J. (1994). Analysis in human immunodeficiency virus type 1 vectors of *cis*-acting sequences that affect gene transfer into human lymphocytes. *J. Virol.* 68, 3888–3895.

Poznansky, M., Lever, A., Bergeron, L., Haseltine, W., and Sodroski, J. (1991). Gene transfer into human lymphocytes by a defective human immunodeficiency virus type 1 vector. *J. Virol.* 65, 532–536.

Purzycka, K. J., Pachulska-Wieczorek, K., and Adamiak, R. W. (2011). The in vitro loose dimer structure and rearrangements of the HIV-2 leader RNA. *Nucleic Acids Res.* 39, 7234–7248.

Rein, A. (1994). Retroviral RNA packaging: a review. *Arch. Virol.* 9, 513–522.

Rizvi, T. A., and Panganiban, A. T. (1993). Simian immunodeficiency virus RNA is efficiently encapsidated by human immunodeficiency virus type 1 particles. *J. Virol.* 67, 2681–2688.

Russell, R. S., Hu, J., Laughrea, M., Wainberg, M. A., and Liang, C. (2002). Deficient dimerization of human immunodeficiency virus type 1 RNA caused by mutations of the u5 RNA sequences. *Virology* 303, 152–163.

Russell, R. S., Liang, C., and Wainberg, M. A. (2004). Is HIV-1 RNA dimerization a prerequisite for packaging? Yes, no, probably? *Retrovirology* 1, 23.

Sakuragi, J., Iwamoto, A., and Shioda, T. (2002). Dissociation of genome dimerization from packaging functions and virion maturation of human immunodeficiency virus type 1. *J. Virol.* 76, 959–967.

Sakuragi, J., Sakuragi, S., and Shioda, T. (2007). Minimal region sufficient for genome dimerization in the human immunodeficiency virus type 1 virion and its potential roles in the early stages of viral replication. *J. Virol.* 81, 7985–7992.

Sakuragi, J., Shioda, T., and Panganiban, A. T. (2001). Duplication of the primary encapsidation and dimer linkage region of human immunodeficiency virus type 1 RNA results in the appearance of monomeric RNA in virions. *J. Virol.* 75, 2557–2565.

Sakuragi, J., Ueda, S., Iwamoto, A., and Shioda, T. (2003). Possible role of dimerization in human immunodeficiency virus type 1 genome RNA packaging. *J. Virol.* 77, 4060–4069.

Sandefur, S., Smith, R. M., Varthakavi, V., and Spearman, P. (2000). Mapping and characterization of the N-terminal I domain of human immunodeficiency virus type 1 Pr55(Gag). *J. Virol.* 74, 7238–7249.

Skripkin, E., Paillart, J. C., Marquet, R., Ehresmann, B., and Ehresmann, C. (1994). Identification of the primary site of the human immunodeficiency virus type 1 RNA dimerization in vitro. *Proc. Natl. Acad. Sci. U.S.A.* 91, 4945–4949.

Spriggs, S., Garyu, L., Connor, R., and Summers, M. F. (2008). Potential intra- and intermolecular interactions involving the unique-5′ region of the HIV-1 5′-UTR. *Biochemistry* 47, 13064–13073.

Summers, M. F., Henderson, L. E., Chance, M. R., Bess, J. W., South, T. L., Blake, P. R., Sagi, I., Perez-Alvarado, G., Sowder, R. C., and Hare, D. R. (1992). Nucleocapsid zinc fingers detected in retroviruses: EXAFS studies of intact viruses and the solution-state structure of the nucleocapsid protein from HIV-1. *Protein Sci.* 1, 563–574.

Summers, M. F., South, T. L., Kim, B., and Hare, D. R. (1990). High-resolution structure of an HIV zinc fingerlike domain via a new NMR-based distance geometry approach. *Biochemistry* 29, 329–340.

Tounekti, N., Mougel, M., Roy, C., Marquet, R., Darlix, J. L., Paoletti, J., Ehresmann, B., and Ehresmann, C. (1992). Effect of dimerization on the conformation of the encapsidation Psi domain of Moloney murine leukemia virus RNA. *J. Mol. Biol.* 223, 205–220.

Tsukahara, T., Komatsu, H., Kubo, M., Obata, F., and Tozawa, H. (1996). Binding properties of human immunodeficiency virus type-2 (HIV-2) RNA corresponding to the packaging signal to its nucleocapsid protein. *Biochem. Mol. Biol. Int.* 40, 33–42.

Watanabe, S., and Temin, H. M. (1982). Encapsidation sequences for spleen necrosis virus, an avian retrovirus, are between the 5′ long terminal repeat and the start of the gag gene. *Proc. Natl. Acad. Sci. U.S.A.* 79, 5986–5990.

Watts, J. M., Dang, K. K., Gorelick, R. J., Leonard, C. W., Bess, J. W., Swanstrom, R., Burch, C. L., and Weeks, K. M. (2009). Architecture and secondary structure of an entire HIV-1 RNA genome. *Nature* 460, 711–716.

Wilkinson, K. A., Gorelick, R. J., Vasa, S. M., Guex, N., Rein, A., Mathews, D. H., Giddings, M. C., and Weeks, K. M. (2008). High-throughput SHAPE analysis reveals structures in HIV-1 genomic RNA strongly conserved across distinct biological states. *PLoS Biol.* 6, e96. doi:10.1371/journal.pbio.0060096

Yu, S. S., Kim, J. M., and Kim, S. (2000). The 17 nucleotides downstream from the env gene stop codon are important for murine leukemia virus packaging. *J. Virol.* 74, 8775–8780.

Conflict of Interest Statement: The authors declare that the research was conducted in the absence of any commercial or financial relationships that could be construed as a potential conflict of interest.

Received: 28 November 2011; paper pending published: 08 December 2011; accepted: 11 December 2011; published online: 29 December 2011.

Citation: Miyazaki Y, Miyake A, Nomaguchi M and Adachi A (2011) Structural dynamics of retroviral genome and the packaging. Front. Microbio. 2:264. doi: 10.3389/fmicb.2011.00264

This article was submitted to Frontiers in Virology, a specialty of Frontiers in Microbiology.

OPEN ACCESS Freely available online

PLoS one

A Single Amino Acid of Human Immunodeficiency Virus Type 2 Capsid Protein Affects Conformation of Two External Loops and Viral Sensitivity to TRIM5α

Tadashi Miyamoto[1], Masaru Yokoyama[2], Ken Kono[1,3], Tatsuo Shioda[1], Hironori Sato[2], Emi E. Nakayama[1]*

1 Department of Viral infections, Research Institute for Microbial Diseases, Osaka University, Suita, Osaka, Japan, **2** Pathogen Genomics Center, National Institute of Infectious Diseases, Musashi Murayama, Tokyo, Japan, **3** Research Fellow of the Japan Society for the Promotion of Science, Tokyo, Japan

Abstract

We previously reported that human immunodeficiency virus type 2 (HIV-2) carrying alanine or glutamine but not proline at position 120 of the capsid protein (CA) could grow in the presence of anti-viral factor TRIM5α of cynomolgus monkey (CM). To elucidate details of the interaction between the CA and TRIM5α, we generated mutant HIV-2 viruses, each carrying one of the remaining 17 possible amino acid residues, and examined their sensitivity to CM TRIM5α-mediated restriction. Results showed that hydrophobic residues or those with ring structures were associated with sensitivity, while those with small side chains or amide groups conferred resistance. Molecular dynamics simulation study revealed a structural basis for the differential TRIM5α sensitivities. The mutations at position 120 in the loop between helices 6 and 7 (L6/7) affected conformation of the neighboring loop between helices 4 and 5 (L4/5), and sensitive viruses had a common L4/5 conformation. In addition, the common L4/5 structures of the sensitive viruses were associated with a decreased probability of hydrogen bond formation between the 97th aspartic acid in L4/5 and the 119th arginine in L6/7. When we introduced aspartic acid-to-alanine substitution at position 97 (D97A) of the resistant virus carrying glutamine at position 120 to disrupt hydrogen bond formation, the resultant virus became moderately sensitive. Interestingly, the virus carrying glutamic acid at position 120 showed resistance, while its predicted L4/5 conformation was similar to those of sensitive viruses. The D97A substitution failed to alter the resistance of this particular virus, indicating that the 120th amino acid residue itself is also involved in sensitivity regardless of the L4/5 conformation. These results suggested that a hydrogen bond between the L4/5 and L6/7 modulates the overall structure of the exposed surface of the CA, but the amino acid residue at position 120 is also directly involved in CM TRIM5α recognition.

Citation: Miyamoto T, Yokoyama M, Kono K, Shioda T, Sato H, et al. (2011) A Single Amino Acid of Human Immunodeficiency Virus Type 2 Capsid Protein Affects Conformation of Two External Loops and Viral Sensitivity to TRIM5α. PLoS ONE 6(7): e22779. doi:10.1371/journal.pone.0022779

Editor: Young-Min Lee, Chungbuk National University, Korea, Republic of

Received February 7, 2011; **Accepted** July 7, 2011; **Published** July 28, 2011

Funding: This work was supported by grants from the Health Science Foundation, the Ministry of Education, Culture, Sports, Science, and Technology, and the Ministry of Health, Labour and Welfare, Japan. The funders had no role in study design, data collection and analysis, decision to publish, or preparation of the manuscript.

Competing Interests: The authors have declared that no competing interests exist.

* E-mail: emien@biken.osaka-u.ac.jp

Introduction

Human immunodeficiency virus type 1 (HIV-1) infects humans and chimpanzees but not Old World Monkeys (OWM) such as Rhesus monkey (Rh) and cynomolgus monkey (CM). This is attributed to a barrier in the host cell. In 2004, the screening of a Rh cDNA library identified TRIM5α as one of cellular antiviral factors [1]. TRIM5 is a member of the tripartite motif family containing RING, B-box and coiled-coil domains [2]. The alpha isoform of TRIM5 has an additional C-terminal PRYSPRY (B30.2) domain. Several studies have shown that sequence variation in variable regions of the PRYSPRY domain among different monkey species affects species-specific retrovirus infection [3–11].

Rh and CM TRIM5αs restrict HIV-1 but not simian immunodeficiency virus isolated from macaque (SIVmac) [1,5], whereas African green monkey (AGM) TRIM5α inhibits both HIV-1 and SIVmac [5,12]. Human TRIM5α only weakly restricts HIV-1, but potently restricts N-tropic murine leukemia virus (N-MLV) [11,12].

Details of the molecular mechanism of retrovirus restriction by TRIM5α have been gradually elucidated by several groups. TRIM5α associates with the N-MLV capsid in detergent-stripped virions [13] or with an artificially constituted core structure composed of an HIV-1 capsid-nucleocapsid (CA-NC) fusion protein in a PRYSPRY domain-dependent manner [14], indicating that the target of TRIM5α is multimerized capsids. In addition, it was demonstrated that engagement of a restriction-sensitive retroviral core results in TRIM5α degradation by a proteasome-dependent pathway [15]. In the presence of proteasome inhibitors, virions complete reverse transcription and form functional pre-integration complexes, but 2-long terminal repeat circle formation and gene expression remain impaired [16,17]. Recently, we have reported that AGM TRIM5α restricted SIVmac mainly via the proteasome-dependent pathway, whereas HIV-1 and HIV-2 restriction by AGM TRIM5α was both proteasome-dependent and proteasome-independent [18].

HIV-2 and SIVmac have very similar genomes [19], but vary in their ability to grow in the presence of TRIM5α from various

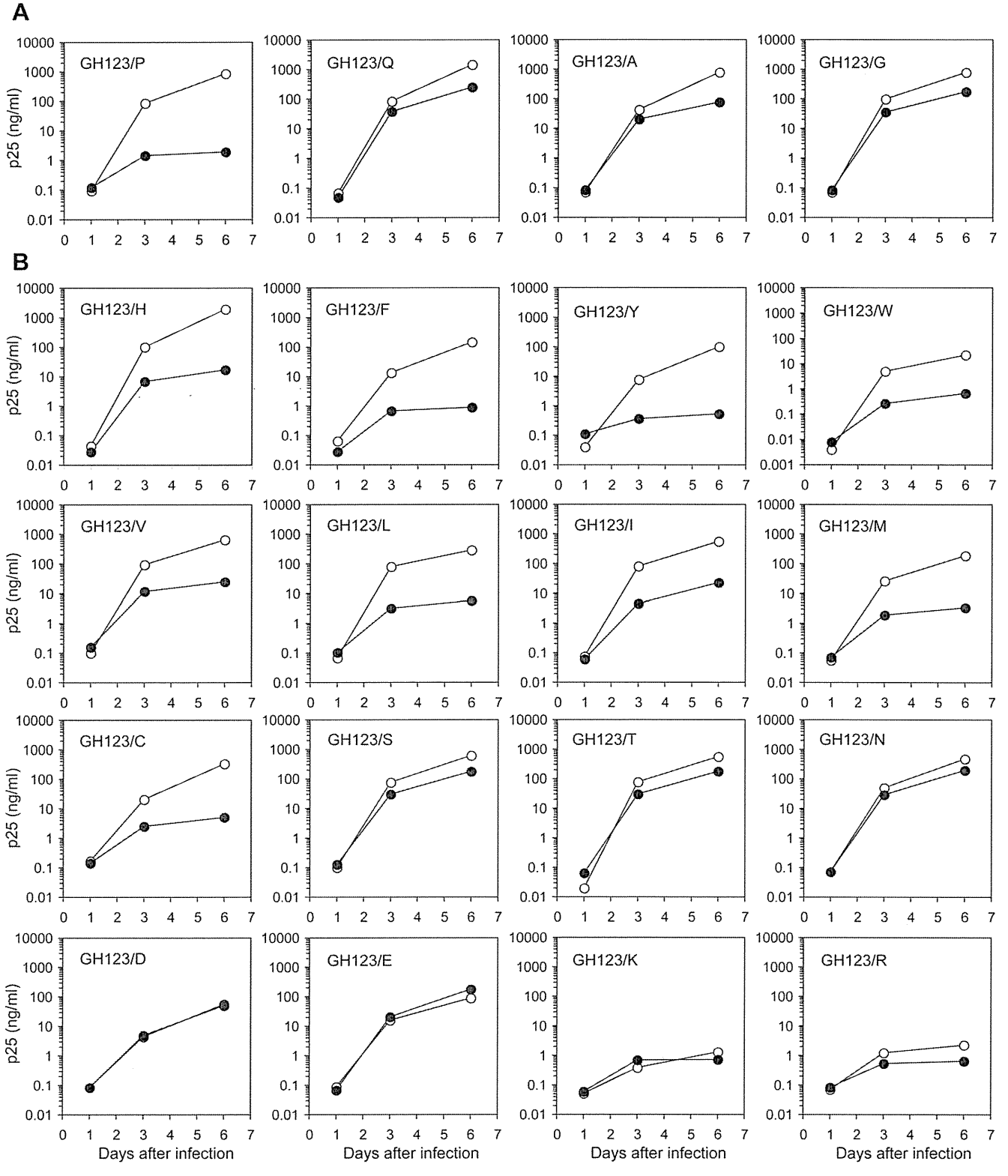

Figure 1. Growth of GH123 and its mutant viruses in the presence of CM TRIM5α. MT4 cells were infected with CM-TRIM5α-SeV (black circles) or CM-SPRY(–)-SeV (white circles) then superinfected with GH123 mutant viruses. Culture supernatants were periodically assayed for levels of virus capsid. Error bars show actual fluctuations between measurements of capsid in duplicate samples. A representative of two independent experiments is shown.
doi:10.1371/journal.pone.0022779.g001

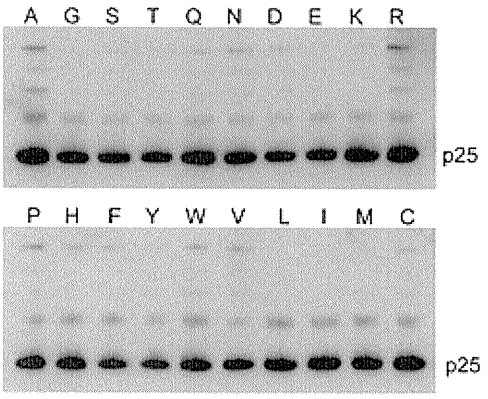

Figure 2. Western blot analysis of the CA in particles of GH123 and its mutant viruses. The viral particles of GH123 wild type and its mutant viruses were purified by ultracentrifugation through a 20% sucrose cushion. p25 capsid protein was visualized by western blotting (WB) using SIV-infected monkey serum.
doi:10.1371/journal.pone.0022779.g002

species. SIVmac239 is resistant to Rh and CM TRIM5αs [1,5,8], whereas HIV-2 strains GH123 and ROD are sensitive to these TRIM5αs [5,8,20,21]. We previously investigated the growth of eight different HIV-2 isolates in the presence of CM and human TRIM5αs and demonstrated that the growth of HIV-2 isolates carrying proline (P) at the 119th or 120th position of the capsid protein (CA) was inhibited by CM and human TRIM5αs, whereas the growth of those with either alanine (A) or glutamine (Q) was not affected by these TRIM5αs [20]. In a Caio cohort study in west Africa, it was demonstrated that subjects with a lower viral load more frequently carried a P at the 119th position of the CA, which corresponds to the 120th position of the GH123 CA, while non-proline residues at this position were more frequently observed in subjects with a high viral load [22], suggesting that TRIM5α controls viral replication in HIV-2-infected individuals.

The 120th amino acid is located in the loop between helices 6 and 7 (L6/7) [20]. Recently, we have succeeded in improving the replication of simian-tropic HIV-1 in CM cells by introducing the SIVmac L6/7 CA sequence [23]. In the present study, we generated mutant HIV-2 viruses each carrying one of the remaining 17 possible amino acid residues at the 120th position, and examined their susceptibilities to TRIM5α-mediated restriction in order to elucidate details of the interaction between HIV-2 CA and TRIM5α. Computer-assisted structural study showed that the mutations at position 120 in L6/7 affected conformation of the neighboring loop between helices 4 and 5 (L4/5).

Results

Amino acid residues at the 120th position of HIV-2 GH123 CA and viral susceptibility to CM TRIM5α

In a previous study, we reported that HIV-2 isolates carrying P at the 120th position of the CA were sensitive to CM and human TRIM5αs, whereas those with either A or Q were not [20]. In the Los Alamos sequence database, the amino acid residue at the 119th or 120th position of almost all HIV-2 CAs is P, A, Q or glycine (G). Therefore, we first generated mutant HIV-2 GH123 viruses carrying G at the 120th position (GH123/G) to investigate its effect on TRIM5α susceptibility.

Equal amounts of p25 of mutant and wild type viruses were inoculated into the human T cell line MT4 expressing CM TRIM5α, and culture supernatants were periodically assayed for CA production. In agreement with the results of the previous study, wild type GH123 carrying P at the 120th position (GH123/P) was sensitive to CM TRIM5α since this virus failed to grow in the presence of CM TRIM5α. On the other hand, GH123/G as well as GH123/Q (glutamine) and GH123/A (alanine) were

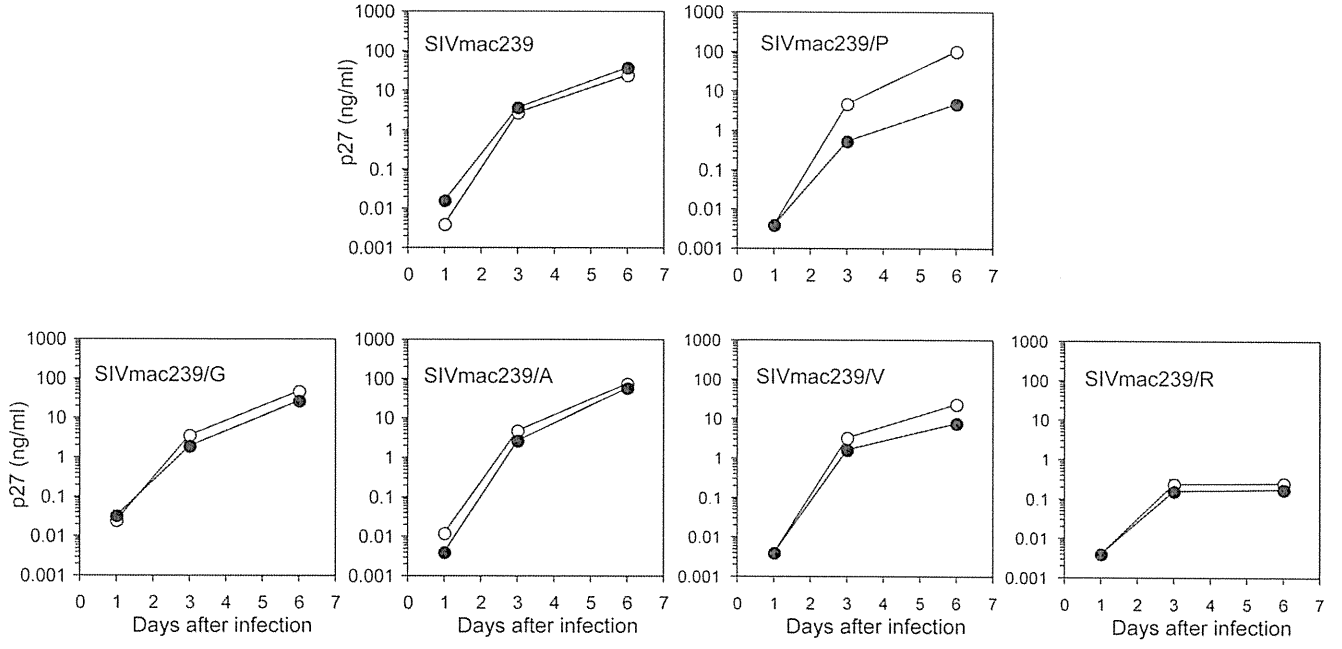

Figure 3. Growth of SIVmac239 and its mutant viruses in the presence of CM TRIM5α. MT4 cells were infected with CM-TRIM5α-SeV (black circles) or CM-SPRY(–)-SeV (white circles) then superinfected with SIVmac239 mutant viruses. Culture supernatants were periodically assayed for levels of virus capsid. Error bars show actual fluctuations between measurements of capsid in duplicate samples. A representative of three independent experiments is shown.
doi:10.1371/journal.pone.0022779.g003

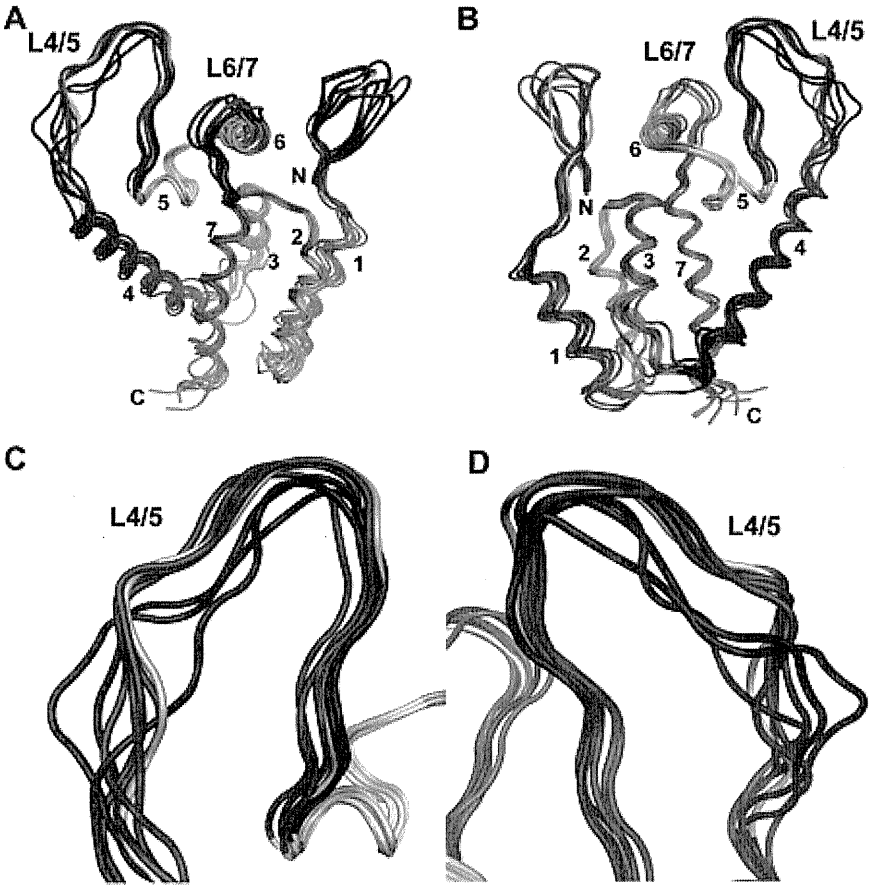

Figure 4. Structural models of the HIV-2 capsid N-terminal domain. Models were constructed by homology modeling and molecular dynamics simulations with the high-resolution X-ray crystal structure of the HIV-2 capsid N-terminal domain (PDB code: 2WLV [29]) as the starting structure. Averaged conformations of the overall structure of the N-terminal domain during 5–20 nanoseconds of MD simulations (A and B) and a close-up view around the L4/5 loop (C and D) are indicated. *N* and *C* indicate the amino termini and carboxyl termini, respectively; and the seven color-coded α-helices are labeled. Red and blue cartoons indicate the N-terminal loop, L4/5, and L6/7 of CM TRIM5α-sensitive (GH123/P, GH123/F, GH123/H and GH123/I) and CM TRIM5α-resistant (GH123/Q, GH123/A and GH123/N) viruses, respectively. Gray cartoons indicate the N-terminal loop, L4/5 and L6/7 of GH123/E in which the structures and biologic phenotypes are inconsistent. Models from two different angles are shown.
doi:10.1371/journal.pone.0022779.g004

resistant to CM TRIM5α, since these viruses could grow in the presence of CM TRIM5α (Figure 1A).

To determine whether amino acid residues other than P, Q, A and G can occupy the 120th position of HIV-2 GH123 CA, and to elucidate further details of the interaction between the CA and TRIM5α, we generated 16 mutant GH123 viruses each carrying one of the remaining possible amino acid residues at the 120th position. As shown in Figure 1B, viruses with amino acid residues bearing a ring structure including aromatic groups, namely, histidine (GH123/H), phenylalanine (GH123/F), tyrosine (GH123/Y), tryptophan (GH123/W) and GH123/P were all sensitive to CM TRIM5α. Hydrophobic valine (GH123/V), leucine (GH123/L), and isoleucine (GH123/I) viruses as well as sulfated methionine (GH123/M) and cysteine (GH123/C) viruses were also sensitive.

In contrast, viruses with amino acid residues bearing hydroxyl or amide groups, namely, serine (GH123/S), threonine (GH123/T), glutamine (GH123/Q) and asparagine (GH123/N) were resistant to CM TRIM5α. Acidic aspartic acid (GH123/D) and glutamic acid (GH123/E) viruses were also resistant, although they grew to slightly lower titers than wild type GH123/P in the absence of CM TRIM5α. The replication of viruses with basic arginine (GH123/R) and lysine (GH123/K) was severely impaired and it was impossible to evaluate the effects of these residues on susceptibility to TRIM5α. Almost identical results were obtained when we inoculated equal amounts of reverse transcriptase of mutant and wild type GH123 (data not shown). Thus, the nature of the 120th amino acid residue greatly affects viral sensitivity to CM TRIM5α.

CA processing is not affected by the 120th mutation

To understand why GH123/R and GH123/K failed to replicate even in the absence of TRIM5α, we examined the Gag processing of mutant and wild type HIV-2 GH123 viruses using western blot analysis of viral particles. As shown in Figure 2, all mutant HIV-2 GH123 viruses produced viral particles with processed Gag proteins similar to the wild type virus. These results clearly exclude the possibility that the impaired replication of GH123/K and GH123/R viruses were due to inefficient processing of Gag precursors.

The 118th position of SIVmac239 CA and viral susceptibility to CM TRIM5α

HIV-2, simian immunodeficiency virus isolated from sooty mangabey (SIVsm), and SIVmac have similar genomes [19]. SIVmac239 can replicate in the presence of CM TRIM5α [5] and

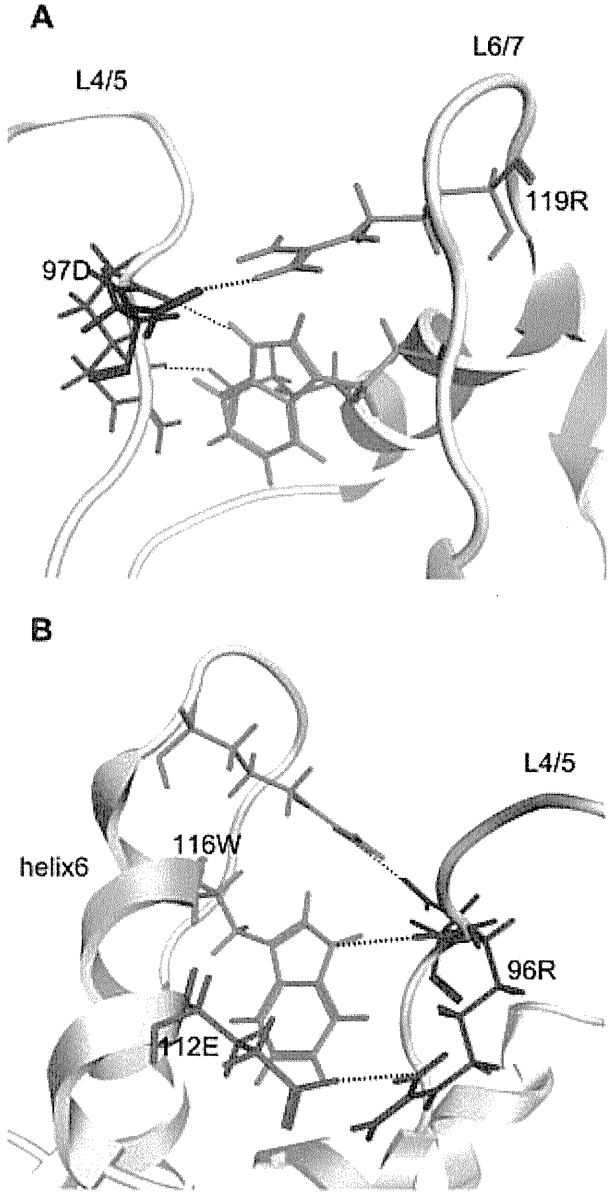

Figure 5. Hydrogen bond formation among L4/5, L6/7 and helix 6 of the HIV-2 CA. Close-up views of averaged structures of the N-terminal domain of the GH123/P CA during 5–20 nanoseconds of MD simulations are shown. Red, blue, purple, orange and green wireframes denote side chains of arginine at the 96th (96R), aspartic acid at the 97th (97D), glutamic acid at the 112th (112E), tryptophan at the 116th (116W) and arginine at the 119th (119R) positions, respectively. Dotted lines indicate hydrogen bonds visualized with MOE 2009. Models from two different angles are shown.
doi:10.1371/journal.pone.0022779.g005

contains Q at the 118th position, which corresponds to the 120th position of the GH123 CA. In our previous study, we reported that mutant SIVmac239 carrying P at the 118th position (SIVmac239/P) became sensitive to CM and human TRIM5αs [20]. In the present study, we examined whether other amino acid residues that conferred resistance (A, G) or sensitivity (valine, V) to CM TRIM5α or abolished viral replicative ability (arginine, R) on a GH123 background showed similar effects on viral sensitivity to CM TRIM5α on an SIVmac239 background.

As shown in Figure 3, CM TRIM5α did not affect the replication of wild type SIVmac239 but inhibited SIVmac239/P, which is in agreement with the results of the previous study [20]. It should be noted, however, that the inhibitory effect of CM TRIM5α on SIVmac239/P was smaller than that on GH123/P, since SIVmac239/P demonstrated some growth even in the presence of CM TRIM5α. Newly generated SIVmac239 carrying alanine (SIVmac239/A) or glycine (SIVmac239/G) at the 118th position were unaffected by CM TRIM5α (Figure 3).

On the other hand, the mutant SIVmac239 carrying valine (SIVmac239/V) was only weakly inhibited by CM TRIM5α (Figure 3) to a lesser degree than the GH123/V. As shown in Figure 1, the inhibitory effect on GH123/V was also smaller than that on GH123/P even on a GH123 background. These results clearly indicate that single amino acid substitutions at the 118th position of the SIVmac239 CA had similar effects to those at the 120th position of GH123, although their impact was smaller in SIVmac239 than in the GH123 CA. Nevertheless, replication of mutant SIVmac239 carrying arginine (SIVmac239/R) was severely impaired, as with GH123/R.

Molecular modeling and molecular dynamics (MD) simulations of the HIV-2 capsid N-terminal domain

The amino acid at position 120 is located in the L6/7 of the N-terminal domain of the CA. To obtain structural insights into the mechanisms by which this amino acid controls viral sensitivity to TRIM5α-mediated restriction, we conducted computer-assisted structural study of the N-terminal domain of the CA. With homology modeling and molecular dynamics (MD) simulation techniques, we constructed a series of initial structural models of the N-terminal half of the CA from CM TRIM5α-sensitive (GH123/P, GH123/F, GH123/H, and GH123/I) and CM TRIM5α-resistant (GH123/Q, GH123/A, GH123/N, and GH123/E) viruses. The initial models were then subjected to the MD simulation to analyze structural dynamics of the N-terminal domain of the CA in water environment. Average structures of individual CA mutants were obtained with 60,000 trajectories during 5–20 nanoseconds of MD simulations.

Comparisons of the average structures revealed that amino acid substitutions at position 120 could significantly influence the overall conformation of the exposed surface of the HIV-2 CA (Figure 4). Notably, the L4/5 of the mutant CAs are classified into two subgroups on the basis of their conformational similarities. These subgroups are primarily coincident with the two phenotypic subgroups based on viral sensitivities to CM TRIM5α, with the exception of mutant GH123/E (Figure 4, cartoon models indicated by gray). TRIM5α-sensitive viruses GH123/P, GH123/F, GH123/H and GH123/I showed almost identical L4/5 conformation (Figure 4, red models), while L4/5 of TRIM5α-resistant viruses GH123/Q, GH123/A and GH123/N were more variable (Figure 4, blue models). To confirm this, we performed additional modeling of TRIM5α-resistant viruses GH123/T and GH123/S. The results showed that L4/5 of GH123/T and GH123/S were also variable (data not shown).

Furthermore, the MD simulation study revealed that the common L4/5 structures of the TRIM5α-sensitive viruses were associated with a reduced probability of hydrogen bond formation between the 97th aspartic acid (D) in L4/5 and the 119th arginine (R) in L6/7 compared with those of TRIM5α-resistant viruses except for GH123/E (Figure 5A and Table 1). We, therefore, hypothesized that the presence of the hydrogen bond between the 97th D in L4/5 and the 119th R in L6/7 disrupted the L4/5 conformation required for recognition by TRIM5α. To examine whether hydrogen bond formation between the 97th D and 119th R indeed affects the viral sensitivity to CM TRIM5α-mediated restriction, we introduced an alanine substitution at the 97th